

Title Page

Title: Consumption of atmospheric H₂ during the life cycle of soil-dwelling actinobacteria

Authors: Laura K. Meredith^{1,4}, Deepa Rao^{1,5}, Tanja Bosak¹, Vanja Klepac-Ceraj², Kendall R. Tada², Colleen M. Hansel³, Shuhei Ono¹, and Ronald G. Prinn¹

(1) Massachusetts Institute of Technology, Department of Earth, Atmospheric and Planetary Science, Cambridge, Massachusetts, 02139, USA.

(2) Wellesley College, Department of Biological Sciences, Wellesley, Massachusetts, 02481, USA.

(3) Woods Hole Oceanographic Institution, Department of Marine Chemistry and Geochemistry, Woods Hole, Massachusetts, 02543, USA.

Corresponding author:

Laura K. Meredith

Address: 77 Massachusetts Ave., 54-1320, Cambridge, MA, 02139

Telephone: (617) 253-2321

Fax: (617) 253-0354

Email: predawn@mit.edu

Running title: Uptake of H₂ during the life cycle of soil actinobacteria

Summary

Microbe-mediated soil uptake is the largest and most uncertain variable in the budget of atmospheric hydrogen (H₂). The diversity and ecophysiological role of soil microorganisms that can consume low atmospheric abundances of H₂ with high-affinity [NiFe]-hydrogenases is

Author current addresses: (4) Stanford University, Environmental Earth System Science, Palo Alto, CA, 94305, USA. (5) Georgetown University, Communication, Culture and Technology, Washington, DC, 20057.

22 unknown. We expanded the library of atmospheric H₂-consuming strains to include four soil
23 Harvard Forest Isolate (HFI) *Streptomyces* spp., *Streptomyces cattleya*, and *Rhodococcus equi* by
24 assaying for high-affinity hydrogenase (*hhyL*) genes and quantifying H₂ uptake rates. We find
25 that aerial structures (hyphae and spores) are important for *Streptomyces* H₂ consumption; uptake
26 was not observed in *Streptomyces griseoflavus* Tu4000 (deficient in aerial structures) and was
27 reduced by physical disruption of *Streptomyces* sp. HFI8 aerial structures. H₂ consumption
28 depended on the life cycle stage in developmentally distinct actinobacteria: *Streptomyces* sp.
29 HFI8 (sporulating) and *R. equi* (non-sporulating, non-filamentous). Strain HFI8 took up H₂ only
30 after forming aerial hyphae and sporulating, while *R. equi* only consumed H₂ in the late
31 exponential and stationary phase. These observations suggest that conditions favoring H₂ uptake
32 by actinobacteria are associated with energy and nutrient limitation. Thus, H₂ may be an
33 important energy source for soil microorganisms inhabiting systems in which nutrients are
34 frequently limited.

35 Main Text

36 Introduction

37 Microbe-mediated soil uptake is the leading driver of variability in atmospheric H₂ and accounts
38 for 60% to 90% of the total H₂ sink; however, the dependence of this sink on environmental
39 parameters is poorly constrained by field and lab measurements (Xiao et al., 2007; recently
40 reviewed by Ehhalt and Rohrer, 2009). Atmospheric H₂ is an abundant reduced trace gas (global
41 average of 530 ppb) that influences the atmospheric chemistry of the troposphere and the
42 protective stratospheric ozone layer (Novelli et al., 1999). Most notably, the reaction of H₂ with
43 the hydroxyl radical ($\bullet\text{OH}$) attenuates the amount of $\bullet\text{OH}$ available to scavenge potent
44 greenhouse gases, like methane (CH₄), from the atmosphere. The H₂ soil sink may play a

45 considerable role in buffering anthropogenic H₂ emissions, which constitute approximately 50%
46 of atmospheric H₂ sources (Ehhalt and Rohrer, 2009). A process-level understanding of the H₂
47 soil sink is required to understand the natural variability of atmospheric H₂ and its sensitivity to
48 changes in climate and anthropogenic activities.

49 Early studies established the H₂ soil sink as a biological process because of the enzymatic
50 nature of H₂ consumption (Conrad and Seiler, 1981; Schuler and Conrad, 1990; Häring and
51 Conrad, 1994). Initially, free soil hydrogenases were thought to be the primary drivers of the H₂
52 soil sink because chemical fumigation of soils had little effect on soil H₂ uptake rates but
53 significantly reduced the active microbial consumption or production of other trace gases, *e.g.*,
54 the active microbial uptake of CO (Conrad and Seiler, 1981; Conrad et al., 1983b; Conrad,
55 1996). Only indirect evidence existed to support the notion that the soil sink was an active
56 microbial process (Conrad and Seiler, 1981; Conrad et al. 1983a; King, 2003b) until the isolation
57 of *Streptomyces* sp. PCB7, the first microorganism to exhibit significant consumption of
58 atmospheric H₂ (Constant et al., 2008). This organism demonstrated high-affinity ($K_m \sim 10\text{-}50$
59 ppm), low-threshold (< 0.1 ppm) H₂ uptake kinetics characteristic of uptake by environmental
60 soil samples (Conrad, 1996). Previously, only low-affinity ($K_m \sim 1000$ ppm), high-threshold ($>$
61 0.5 ppm) H₂-oxidizing microorganisms were characterized, which were unable to consume H₂ at
62 atmospheric concentrations (Conrad et al., 1983b; Conrad, 1996; Guo and Conrad, 2008;
63 summarized by Constant et al., 2009).

64 *Streptomyces* spp. are ubiquitous soil microorganisms that degrade recalcitrant materials
65 in soils (Kieser et al., 2000). Theoretically, the observed rates of atmospheric H₂ soil
66 consumption can sustain the maintenance energy requirements for typical numbers of
67 *Streptomyces* spp. cells in soils (Conrad, 1999; Constant et al., 2010; Constant et al., 2011a).

68 However, the importance of atmospheric H₂ as a source of energy to soil microorganisms
69 remains unknown. Atmospheric H₂ uptake was specifically linked to a group 5 [NiFe]-
70 hydrogenase gene cluster containing genes that encode for the small and large hydrogenase
71 subunits, *hhyS* and *hhyL*, respectively (Constant et al., 2010). The *hhyL* gene is distributed
72 unevenly amongst the Actinobacteria, Proteobacteria, Chloroflexi, and Acidobacteria phyla (*e.g.*,
73 many, but not all *Streptomyces* spp. possess the gene) (Constant et al., 2010; Constant et al.,
74 2011b). The link between high-affinity H₂ uptake and *hhyL* has been reported in nine
75 *Streptomyces* spp. and in *Mycobacterium smegmatis* (Constant et al., 2011b; King, 2003b), but it
76 remains untested in many soil microorganisms. Additional research adding to the library of
77 atmospheric H₂-oxidizing bacteria is needed to identify the key microorganisms involved in H₂
78 biogeochemical cycling. Information about the genes and ecophysiology of these organisms can
79 improve the process-level understanding of the H₂ soil sink (Conrad, 1996; Madsen, 2005).

80 The life cycle of *Streptomyces* is complex and controls the timing of many physiological
81 activities, which may include H₂ uptake (Kieser et al., 2000; Schrempf, 2008; Flärdh and
82 Buttner, 2009). In soils, *Streptomyces* exist predominantly as inactive spores, which germinate in
83 response to environmental triggers such as moisture and nutrient availability (Kieser et al., 2000)
84 and grow vegetatively, producing a network of mycelia that grow into the substrate (Flärdh and
85 Buttner, 2009). Over time, and in response to environmental triggers such as nutrient depletion
86 or physiological stresses, the colony differentiates to form hydrophobic aerial hyphae that break
87 the substrate surface tension and grow into the air, forming a millimeter-scale canopy in
88 immediate contact with the atmosphere (Kieser et al., 2000; Schrempf, 2008). Finally, aerial
89 hyphae differentiate and septate to form chains of resistant spores (Flärdh and Buttner, 2009). In
90 cultures of *Streptomyces* sp. PCB7 growing on soil particles, H₂ uptake coincided with the

91 presence of aerial hyphae and spores (Constant et al., 2008). It is unknown if H₂ uptake occurs at
92 the same life cycle stage in other *Streptomyces* strains and how long uptake persists in the spore
93 stage. Furthermore, the timing of atmospheric H₂ uptake in microbes that possess *hhyL*, but do
94 not sporulate has not been measured.

95 The goal of this paper is to address two questions. First, our study asks whether
96 environmental isolates and culture collection strains with the genetic potential for atmospheric
97 H₂ uptake, i.e., the *hhyL* gene, actually exhibit atmospheric H₂ uptake. To expand the library of
98 atmospheric H₂-oxidizing bacteria, we quantify H₂ uptake rates by novel *Streptomyces* soil
99 isolates that contain the *hhyL* and by three previously isolated and sequenced strains of
100 actinobacteria whose *hhyL* sequences span the known *hhyL* diversity. Second, we investigate
101 how H₂ uptake varies over organismal life cycle in one sporulating and one non-sporulating
102 microorganism, *Streptomyces* sp. HFI8 and *Rhodococcus equi*, respectively. These experiments
103 probe the advantage of atmospheric H₂ consumption to microbes and relationship between
104 environmental conditions, physiology of soil microbes, and H₂.

105 **Results**

106 **H₂ uptake by microbial soil isolates and culture collection strains possessing *hhyL*.**

107 Candidate *Streptomyces* strains, referred to henceforth as Harvard Forest Isolate (HFI)
108 strains, were isolated from Harvard Forest soils. PCR amplification revealed that *hhyL* encoding
109 the high-affinity [NiFe]-hydrogenase was present in six out of nine tested strains. Four of these
110 strains (HFI6, HFI7, HFI8, and HFI9) were successfully retained in culture and were used to test
111 the link between *hhyL* and H₂ uptake activity. These strains exhibited distinctive *Streptomyces*
112 traits such as pigmentation, a fuzzy appearance indicating the production of aerial hyphae
113 (Figures S1 and S2), and the distinctive earthy scent of geosmin (Schrempf, 2008). The 16S

114 rRNA gene sequences of the new isolates fell within the *Streptomyces* genus and were 100%
115 identical to several different strains of *Streptomyces* spp. (Table S1). Of two clusters that were
116 defined by Constant et al. (2011b) based on a deeply rooted split (99% of bootstrap replicates) in
117 the phylogenetic tree of *hhyL* amino acid sequences (Figure S3), the HFI6 - HFI9 *hhyL*
118 sequences group with *hhyL* Cluster 1. In addition to our *Streptomyces* isolates, we examined
119 three culture collection strains in this study to broaden representation across the *hhyL* clusters
120 and genera (Bergey et al., 1957): *Streptomyces griseoflavus* Tu4000 (Cluster 1), *Rhodococcus*
121 *equi* (Actinobacterium, Cluster 1), and *Streptomyces cattleya* (Cluster 2).

122 (Insert Table 1 here)

123 To test whether organisms with *hhyL* gene sequences consume H₂, we measured the
124 uptake of atmospheric H₂ in sporulated *Streptomyces* cultures and in stationary stage of *R. equi*.
125 The presence of *hhyL* predicted atmospheric H₂ uptake activity in HFI strains 6-9, *S. cattleya*,
126 and *R. equi*, but not in *S. griseoflavus* Tu4000 (Table 1). We find that atmospheric H₂ uptake
127 observed in strains with *hhyL* from Cluster 1 (*Streptomyces* strains HFI6 - HFI9 and *R. equi*) and
128 Cluster 2 (*S. cattleya*). The biomass-weighted H₂ uptake rates of these isolates spanned nearly
129 two orders of magnitude (from 10 to 780 nmol min⁻¹ g⁻¹), and the *Streptomyces* strains that took
130 up H₂ did so at rates more than 10-fold greater than dense stationary phase cultures of *R. equi*
131 (Table 1). *R. equi* consumed atmospheric H₂, both when grown on solid R2A medium and in
132 liquid TSB medium (data not shown). Uptake rates of *Streptomyces* cultures were measured on
133 solid medium because *Streptomyces* cultures typically do not progress through their full
134 developmental cycle in liquid medium (Flärdh and Buttner, 2009). The Michaelis-Menten
135 substrate affinity was determined from the x-intercept of Lineweaver-Burk plots of the inverse
136 relationship between the first-order H₂ uptake rate and initial headspace H₂ concentrations

137 between 0 and 35 ppm. This method can be more error prone than the non-inverse approach
138 performed over a greater range of initial H₂ mole fractions, but it better restricts H₂ uptake by
139 low-affinity hydrogenases, and has enough sensitivity to distinguish high- and low-affinity
140 uptake kinetics. K_m values of HFI strains were typically low (40-80 ppm for HFI strains), which
141 indicated that enzymatic processing of H₂ is tuned to operate efficiently at atmospheric levels of
142 H₂ (high-affinity uptake). *S. cattleya* and *R. equi* appeared have high- or intermediate-affinity K_m
143 values (<1000 ppm), but did not pass the quality control measures (Experimental Procedures) to
144 be included in Table 1. The minimum H₂ concentration, or threshold, consumed by each HFI
145 strain ranged from 0.12 to 0.15 ppm, which is well below typical atmospheric mole fractions of
146 around 0.53 ppm (Table 1). *S. cattleya* and *R. equi* thresholds were also below atmospheric
147 levels at least below 0.45 and 0.30 ppm, respectively (Table 1). This study augments the library
148 of organisms that contain *hhyL* sequences and take up atmospheric H₂ with high-affinity and a
149 low-threshold from 10 to 16 strains.

150 **H₂ uptake correlates with lifecycle stage in *Streptomyces* sp. HFI8**

151 We randomly selected *Streptomyces* sp. HFI8 from our HFI strains as a representative
152 organism to determine whether high-affinity H₂ consumption depended on the stage of the life
153 cycle and how long uptake lasted in the sporulation stage. Microscopy revealed the progression
154 of strain HFI8 through developmental stages over 44 days on solid agar (Figure S4). Following
155 germination, the colonies of strain HFI8 grew as substrate mycelia (Figure S4-A). By day 1.8 the
156 lawn reached its maximal aerial coverage and grew upward as aerial hyphae formed and then
157 sporulated (Figure S4-B). The co-occurrence of partially septated aerial hyphae and spores
158 indicated that the events were not simultaneous throughout the colony (Figure S4-B).
159 Measurements of H₂ uptake revealed that H₂ consumption began only after the formation of

160 aerial hyphae and sporulation around day 2 (Figure 1). Aerial hyphae formation and sporulation
161 are stages of the life cycle often associated with nutrient limitation in *Streptomyces* spp. H₂
162 uptake reached a maximum rate (9.4±2.3 nmol h⁻¹) on day 3.8, two days after sporulation had
163 begun, and then slowly decreased over the next 40 days, dropping below the detection limit of
164 ±0.24 nmol h⁻¹. Most cells between days 2.9 and 44 were a lawn of “dormant” spores that had
165 completed the full life cycle (Figures S4-C-H). H₂ oxidation rates by dormant spores declined
166 slowly over the 44-day experiment to negligible rates (Figure 1). All three replicates displayed
167 similar timing, but the H₂ uptake rates were systematically lower in the third replicate, although
168 the area coverage of the lawn and biomass was not demonstrably different among the replicates.
169 A cursory set of measurements (data not shown) indicated similar trends in H₂ uptake over the
170 life cycle of *Streptomyces* sp. HFI6, *Streptomyces* sp. HFI7, *Streptomyces* sp. HFI9, and *S.*
171 *cattleya*.

172 (Insert Table 2 here)

173 Because the formation of aerial biomass (hyphae and spores) occurred at the same time as
174 the onset of H₂ consumption in *Streptomyces*, we asked whether H₂ uptake activity was
175 physically located in the aerial biomass. We isolated the aerial fraction (spores and aerial
176 hyphae) of strain HFI8 cultures by gently rolling glass beads over the entire surface of the colony
177 and transferring the beads and aerial biomass to an empty, sterile glass vial (Figure S5). H₂
178 uptake rates were measured in whole cultures before the transfer, in the vials with the transferred
179 aerial fraction, and in the original vial with the substrate fraction that remained after the glass
180 bead procedure (Table 2, Samples 1-6; Figure S5). The experiment lasted 2-4 hours following
181 the aerial biomass transfer. H₂ uptake in the transferred aerial biomass fraction was consistently
182 low, typically near or below the limit of detection of ±0.24 nmol h⁻¹, and was thus often

183 statistically indistinguishable from zero. Low uptake rates in the aerial fraction were not the
184 result of poor biomass transfer efficiency by the glass bead procedure; glass beads transferred a
185 significant proportion (Table 2, 0.7 ± 0.6 mg) of the aerial biomass from the replicate cultures of
186 that could be collected using a metal spatula (1.2 ± 0.5 mg). The drop in uptake also cannot be
187 explained by aging over this period, because this occurs over the course of days or weeks and not
188 hours (Figure 1). No reduction in H₂ uptake stemming from reduced spore viability was expected
189 because the biomass transfer procedure by glass beads is based on established methods for
190 harvesting viable spores (*e.g.*, Hirsch and Ensign, 1976; Hardisson et al., 1978). Furthermore, the
191 number of viable spores in bead-treated cultures was indistinguishable from the number of viable
192 spores obtained by transferring aerial biomass by a metal spatula from replicate vials incubated
193 at the same time. This test was done by harvesting spores by the two methods, plating spore
194 suspension dilutions, and counting the number of colony forming units as a function of the initial
195 amount of biomass (protein mass) in the spore suspensions.

196 We found that the net H₂ uptake diminished after the separation of the aerial biomass
197 from the substrate biomass (Table 2). Even in replicates where glass beads were gently rolled
198 over strain HFI8 lawns and all biomass was left in the original vial, net H₂ uptake was
199 significantly reduced (Table 2, Samples 7-12). The larger the initial H₂ oxidation rate, the larger
200 percentage reduction by the glass beads (Figure S6, linear fit, $R^2=0.93$), regardless of culture age
201 or the amount of glass beads used for transfer (Samples 1-12). These experiments suggested that
202 the colony structure and the presence of intact aerial hyphae were important for H₂ uptake.

203 **H₂ uptake correlates with the growth stage of *Rhodococcus equi***

204 (Insert Figure 2 here)

205 Only some microbes containing *hhyL* are sporulating *Streptomyces* (Figure S3). To test
206 whether H₂ uptake by non-sporulating Actinobacterium *R. equi* is related to its lifecycle, we
207 measured the uptake of H₂ by this organism at various stages of growth in liquid cultures (Figure
208 2). The growth phases were determined from optical density measurements of the cultures. *R.*
209 *equi* did not consume measurable quantities of H₂ during the exponential growth phase (day 1 to
210 4), but started taking up H₂ in the late exponential growth phase (day 4 to 7) and in the stationary
211 phase (day 7 to 17) until the end of the experiment (Figure 2). The late exponential phase and
212 stationary phase growth stages are associated with nutrient limitation.

213 The low H₂ uptake rates by *R. equi* were much closer to the experimental detection limit
214 than *Streptomyces* sp. HFI8. This suggested that the lack of uptake could be related to low *R.*
215 *equi* cell densities in late exponential and early stationary phase rather than altered cell
216 physiology. To test this, we concentrated cells from a culture in exponential growth phase (day
217 1.9) into either fresh medium or sterile water to match the cell densities (Figure 2b) of H₂-
218 oxidizing cultures in the late exponential and early stationary phases (comparable to those on
219 days 4-6). In spite of the comparable cell densities, cells concentrated in this manner did not
220 consume H₂ (-0.075 ± 0.15 nmol h⁻¹, Figure 2a). In addition, we diluted cells in stationary phase
221 (day 7.8) into fresh medium or water to obtain suspensions whose cell densities matched those
222 during days 2-3 of the exponential phase (Figure 2). Although H₂ oxidation rates of the
223 exponentially growing cultures on days 2 and 3 were below the limit of detection (± 0.12 nmol h⁻¹),
224 comparably dense cells derived from the diluted stationary phase cultures took up H₂
225 (0.43 ± 0.047 nmol h⁻¹). All cultures were shaken vigorously to ensure the delivery of H₂ into the
226 medium. Some extracellular factors of relevance to H₂ uptake, such as extracellular
227 hydrogenases, may have been carried over into the diluted suspensions. The decrease in the

228 uptake of H₂ by stationary phase cells (74% of undiluted uptake) did not scale with the dilution
229 (22% of the undiluted cell biomass), which corresponds to a relative mismatch factor of 3.5 in H₂
230 uptake versus dilution. The reason is unclear, and could result from H₂ substrate diffusion
231 limitation in very dense cultures, which was partially alleviated upon dilution. If the cultures
232 were diffusion limited for H₂ substrate, the observed H₂ oxidation rate (Table 1) and H₂ uptake
233 rates during late exponential and stationary phases (Figure 2) may underestimate the potential H₂
234 uptake by cultures of *R. equi*. The uptake of H₂ only by stationary phase cells, either in the old
235 culture medium or when resuspended in fresh medium or water, related the uptake of H₂ to the
236 late exponential and stationary phases. Overall, these tests linked *R. equi* H₂ consumption with
237 growth phase.

238 **Discussion**

239 **Link between *hhyL* and H₂ uptake**

240 Our results confirm links between *hhyL* and H₂ uptake to include *R. equi*, four
241 *Streptomyces* HFI soil isolates from Cluster 1, and *S. cattleya* from Cluster 2, thereby providing
242 additional support for the use of the high-affinity hydrogenase gene *hhyL* as a predictor for the
243 capability to consume atmospheric hydrogen. H₂ uptake by *hhyL* by strains from Clusters 1 and 2
244 indicate that the phylogenetic divergence between the two groups does not compromise
245 atmospheric H₂ uptake activity by *hhyL*, or its prediction. Strains HFI6 - HFI9 exhibit high H₂
246 uptake affinities and low uptake thresholds. Culture collection strains exhibit more variable H₂
247 uptake kinetics, in keeping with a recent suggestion that H₂ consuming microorganisms exhibit a
248 continuum of affinities rather than a discrete grouping of high and low affinities (Constant et al.,
249 2010). Current observations of high-affinity H₂ uptake are limited to the *Actinobacteria*, and
250 future studies are required to determine whether H₂ uptake occurs in the other phyla containing

251 the *hhyL* gene, such as Chloroflexi, Planctomycetes, Verrucomicrobia, and Proteobacteria
252 (Figure S3). A genome data-mining investigation revealed the ubiquity of *hhyL* in DNA
253 extracted from forest, desert, agricultural, and peat soils samples, and although some evidence
254 suggests a correlation between soil H₂ uptake rates and the number of H₂-oxidizing bacteria, no
255 correlation was found between *hhyL* DNA copies and soil H₂ uptake rates (Constant et al.,
256 2011a; Constant et al., 2011b). Future work should be aimed both at understanding the diversity
257 and ecophysiology of these *hhyL*-containing microorganisms and at developing methods to
258 predict H₂ uptake activity across ecosystems.

259 **H₂ uptake and the developmental cycle of actinobacteria**

260 Our results support a correlation between the developmental stage of *Streptomyces* spp.
261 and high-affinity H₂ uptake in two ways. First, we did not observe any H₂ uptake in the substrate
262 mycelium developmental phase of *Streptomyces* sp. HFI8. H₂ uptake began only after the
263 formation of aerial hyphae and sporulation. Second, we found that *S. griseoflavus* Tu4000, which
264 grew predominantly as substrate mycelium, did not take up H₂. We propose that the impaired
265 development (i.e. lack of aerial hyphae and/or spores) of *S. griseoflavus* Tu4000 may impair the
266 production or activity of its high-affinity hydrogenase. In culture, *S. griseoflavus* Tu4000 is
267 smooth and waxy, and does not produce the aerial hyphae typical of *Streptomyces* grown on
268 solid culture (Figure S1 and S2). *S. griseoflavus* Tu4000 may belong to a class of *bld* (bald)
269 mutants that are often deficient in aerial hyphae production (Kieser et al., 2000). Sporulation
270 efficiency is also often reduced in *bld* mutants (Szabó and Vitalis, 1992), and *S. griseoflavus*
271 Tu4000 does not form spores on various types of media (J. Blodgett, personal communication),
272 including our cultures. To our knowledge, *S. griseoflavus* Tu4000 is the first *hhyL*-containing
273 *Streptomyces* sp. found to be unable to oxidize atmospheric H₂ under the same experimental

274 conditions that lead to H₂ oxidation by other *Streptomyces* spp. High-affinity H₂ uptake is also
275 absent from Cluster 1 *hhyL* containing cultures of a gram-negative beta-proteobacterium
276 *Ralstonia eutropha* H16 (formerly known as *Alcaligenes eutropha* 16) grown on solid medium
277 and tested for uptake in suspensions (Conrad et al., 1983b). Future experiments could compare
278 sporulating *Streptomyces* with their *bld* mutants or stimulate the formation of aerial hyphae
279 and/or sporulation in *bld* *Streptomyces* spp. mutants by application of exogenous δ -butyrolactone
280 factor (Ueda et al., 2000; Straight and Kolter, 2009), and determine the effect of this stimulation
281 on H₂ oxidation or *hhyL* expression. In summary, the combined lack of aerial hyphae, spores,
282 and H₂ uptake in *S. griseoflavus* Tu4000 and the co-occurrence of these phenotypes in strain
283 HFI8 underscored a strong developmental control of atmospheric H₂ uptake in *Streptomyces*.
284 These observations motivate the use of *Streptomyces* mutants arrested at different points in the
285 developmental cycle to investigate the regulation and physiological role of *hhyL* in sporulating
286 actinobacteria.

287 Our measurements of H₂ uptake in HFI8 colonies disturbed by glass beads indicate that
288 H₂ uptake depends on the physical structure of *Streptomyces* aggregates. Cultures treated by
289 glass beads take up less H₂, suggesting that the activity of the hydrogenase is impaired by the
290 disturbance of the aerial structures. H₂ uptake by the disrupted colony could decrease because of
291 loss in structural support, loss in signaling and nutrient transport within the bacterial lawn
292 (Miguélez et al., 1999), or reduction in the aerial hyphae surface area in contact with the air.
293 Therefore, we attribute the observed decrease in H₂ uptake to physical destruction of the lawn
294 and colony structure of *Streptomyces*.

295 The H₂ uptake by non-sporulating batch cultures of *R. equi* occurs only during late
296 exponential and stationary phase, suggesting that its H₂ consumption may support metabolism

297 under nutrient-limiting conditions. Similarly, H₂ uptake by strain HFI8 is present only during
298 those stages of its life cycle associated with nutrient-limiting conditions, suggesting that H₂ may
299 be an important energy source for *Streptomyces* under stress. This is consistent with previous
300 reports of H₂ oxidation by *M. smegmatis*, a non-sporulating Actinobacterium with a Cluster 1
301 high-affinity [NiFe]-hydrogenase that can persist for many years in host tissue in a nutrient-
302 deprived stationary phase (Smeulders et al, 1999; King, 2003b). *M. smegmatis* expresses the
303 hydrogenase gene under starvation conditions and mutants lacking this hydrogenase have a
304 reduced growth yield under these conditions (Berney and Cook, 2010). Therefore, the ability to
305 scavenge low concentrations of H₂ may be an important adaptation of various sporulating and
306 non-sporulating actinobacteria (Prescott, 1991; Smeulders et al, 1999; Scherr and Nguyen,
307 2009). This could be particularly true in terrestrial environments where nutrient concentrations are
308 often low for extended periods and atmospheric H₂ is available.

309 **Implications for soil H₂ uptake in the environment**

310 Uptake of atmospheric H₂ by spores, which are often considered to be metabolically
311 dormant, may have consequences for both the sporulating microbes and the cycling of H₂ in the
312 environment. H₂ oxidation rates in cultures of strain HFI8 continue to increase for two days after
313 the onset of sporulation. This could reflect heterogeneity in the sample, because not all cells
314 sporulate simultaneously, or maximum H₂ uptake by already formed spores. In any case,
315 measurable H₂ oxidation in sporulated cultures persists for over a month, such that the time-
316 integrated H₂ oxidation in any culture is much larger in spore state than at any other stage in the
317 life cycle. Net H₂ consumption by HFI8 is at least tenfold larger in the spore state (days 4-44)
318 than during the growth of substrate mycelium (through day 1.1) and formation of aerial hyphae
319 (after day 1.8) combined. One should also keep in mind that the H₂ uptake rates measured in

320 culture studies depend on the specific medium, and may not be directly translated to different
321 media or soil types, where the nutritional characteristics, moisture levels, and cell abundances
322 likely differ. The persistence of H₂ oxidation by *Streptomyces* spp. may have consequences for
323 environmental H₂ cycling and environmental conditions that promote the removal of atmospheric
324 H₂. Conditions that favor germination and growth, including soil moisture and nutrient
325 availability (Kieser et al., 2000), may increase the population of *Streptomyces* spp. in the
326 substrate mycelium phase and actually limit the amount of H₂ oxidized by soils. During
327 moisture- or nutrient-limiting conditions, a greater fraction of the population of *Streptomyces*
328 spp. will be in life cycle stages linked with H₂ uptake (aerial hyphae and spores).
329 Counterintuitively, H₂ uptake by *Streptomyces* spp. may be most significant when the
330 environmental conditions are the harshest. H₂ uptake in spores under our experimental conditions
331 is reduced to negligible levels after about a month (Figure 1), indicating that H₂ uptake may be
332 very low in environments where conditions are harsh for long periods, such as deserts.

333 Ultimately, the goal of studying microbial influences on trace gas fluxes is to understand
334 and predict emergent biogeochemical cycling in the environment. This study describes H₂
335 consumption by two developmentally distinct actinobacteria under nutrient-limiting conditions.
336 Field measurements along a chronosequence of recent volcanic deposits support this notion by
337 suggesting that relative uptake of H₂ by the soil microbial community (normalized by soil
338 respiration rates) is most important when soils were limited by organic carbon (King, 2003a).
339 However, insignificant or even opposing trends also exist (Conrad and Seiler, 1985; Rahn et al.,
340 2002), which may be driven by other factors. Future studies are also needed to determine the
341 impact of nutrient- and moisture-limiting conditions on H₂ uptake by soils and to consider the
342 significance and implications of the energetic supply from H₂ for the microorganisms in the

343 competitive soil environment. A better understanding of the process-level controls on microbe-
344 mediated H₂ soil uptake is critical for evaluating the impact of a changing climate on the soil H₂
345 uptake and the impact of continued anthropogenic H₂ emissions on atmospheric chemistry and
346 climate.

347

348 **Experimental Procedures**

349 **Microbial Strains**

350 *Streptomyces* spp. were isolated from soils within the footprint of the Environmental
351 Measurement Site (EMS) atmospheric trace gas flux tower at the Harvard Forest Long Term
352 Ecological Research site in Petersham, MA (42°32'N, 72°11'W). Atmospheric H₂ fluxes were
353 concurrently measured at the same site (Meredith, 2012). Harvard Forest is a mixed deciduous
354 forest with acidic soils originating from sandy loam glacial till (Allen, 1995). Most H₂
355 consumption occurs within the first few centimeters of soil beneath the litter layer (Yonemura et
356 al., 2000; Smith-Downey et al., 2008); therefore, samples were collected from the uppermost six
357 inches of soil after removal of the leaf litter. Sporulating soil organisms such as *Streptomyces*
358 spp. were enriched for using desiccation and chemical destruction (El-Nakeeb and Lechavalier,
359 1963; Schrempf, 2008). Soils were dried for 3-4 hours at 55°C. Dry soil samples (1 g) were
360 ground with a mortar and pestle and were combined with CaCO₃ (1 g). The soil mixtures were
361 incubated for 2 days at 28°C in 100x15 mm polystyrene Petri dishes (sterile, polystyrene,
362 100x15 mm, VWR, Radnor, PA), with moistened filter paper (11.0 cm diameter, Grade 1,
363 Whatman®, Kent, ME) fitted in the lids to maintain a humid environment. After this period,
364 incubated soil mixtures were suspended in 100 ml sterile water and thoroughly vortexed. After

365 settling for 30 min, soil suspensions were serially diluted, and the 10^0 , 10^{-2} , and 10^{-4} dilutions
366 were spread onto R2A plates (Difco™ R2A, BD, Franklin Lakes, NJ) that had been treated with
367 88 mg cycloheximide / L medium (Porter et al., 1960). After incubation at 30°C for 3-5 days,
368 microbial colonies were screened for the presence of any of the following four distinctive
369 *Streptomyces* traits: 1) antibiotic inhibition of neighboring growth (*i.e.*, zone of clearing), 2) a
370 fuzzy appearance indicating the production of aerial hyphae (Figures S1 and S2), 3)
371 pigmentation, or 4) the distinctive earthy scent of geosmin (Schrempf, 2008). Those exhibiting
372 any of the traits were serially transferred onto fresh R2A plates until pure isolates were obtained.
373 The resulting set of isolates, henceforth referred to as Harvard Forest Isolates (HFI), was
374 maintained in culture on R2A agar at room temperature. Strains HFI6, HFI7, HFI8, and HFI9
375 were deposited to the United States Department of Agriculture NRRL Culture Collection for
376 preservation as NRRL B-24941, NRRL B-24943, NRRL B-24942, and NRRL B-24940,
377 respectively.

378 Strains from culture collections that were used in this study have published genomes
379 accessible in the National Center for Biotechnology Information (NCBI) databases
380 (<http://www.ncbi.nlm.nih.gov/>). *Streptomyces griseoflavus* Tu4000 (accession NZ GG657758)
381 was kindly provided by the genome authors and collaborators (Michael Fischbach, John Clardy,
382 Joshua Blodgett). The following strains were obtained from culture collections: *Rhodococcus*
383 *equi* ATCC 33707™ (accession CM001149) and *Streptomyces cattleya* NRRL 8057 (accession
384 NC 016111).

385 **DNA extraction and PCR amplification**

386 DNA was extracted using the PowerSoil® DNA Extraction Kit (MoBio Laboratories,
387 Carlsbad, CA) from colonies. PCR amplification of 16S rRNA and *hhyL* genes, respectively, was

388 performed using a Mastercycler[®] pro (Eppendorf, Hamburg, Germany) in 25 µl reaction volumes
389 with the following reaction mixture: 12.125 µl ddH₂O, 1.25 µl BSA (Roche, Indianapolis, IN),
390 2.5 µl 10x Ex Taq Buffer (TaKaRa), 0.125 (5 units/ µl) Ex Taq (TaKaRa), 2 µl dNTP (2.5 mM
391 TaKaRa), 2.5 µl of each primer suspended at 3µM (IDT, Coralville, IA). The 16S rRNA gene
392 was amplified using universal primers 27F:5'-AGA GTT TGA TCC TGG CTC AG-3' and
393 1492R:5'-ACG GCT ACC TTG TTA CGA CTT-3' (Lane, 1991), and *hhyL* gene was amplified
394 using NiFe244F:5' - GGG ATC TGC GGG GAC AAC CA -3' and NiFe-1640R:5'-TGC ACG
395 GCG TCC TCG TAC GG -3' (Constant et al., 2010). The following program was used: 5 min
396 initial denaturation at 95°C, followed by 30 cycles consisting of 30 s template denaturation at
397 95°C, 30 s hold at the primer annealing temperature, 1.5 min extension at 72°C, and a final
398 extension at 72°C for 5 min. Annealing temperatures of 50°C and 60.7°C were used for the
399 amplification of the 16S rRNA and *hhyL* genes, respectively. The *hhyL* annealing temperature
400 was optimized over a temperature gradient spanning eight temperatures between 50°C and
401 62.2°C using *S. griseoflavus* Tu4000 DNA as template.

402 Each HFI strain was evaluated for the presence of a putative group 5 [NiFe]-hydrogenase
403 by gel electrophoresis of the *hhyL* gene PCR reaction product. Gels were cast (1% agarose, 5µl
404 GelRed nucleic acid stain (Biotum, Hayward, CA)), loaded (5µl PCR product and 2µl DNA
405 loading dye (Fermentas, Glen Burnie, MD)), run (100 V for 1 hr), and visualized (UVP
406 MultiDoc-It™ Digital Imaging System (UVP, Upland, CA)) to verify successful PCR
407 amplification. Migration of HFI strain PCR product was compared to the *S. griseoflavus* Tu4000
408 *hhyL* gene as a positive control and to the DNA Molecular Weight Marker X (Roche,
409 Indianapolis, IN) ladder for reference.

410 **Gene sequencing and sequence analysis**

411 PCR products were sequenced at Genewiz (Cambridge, MA) following the
412 manufacturer's sample preparation guidelines. Both 16S rRNA and *hhyL* gene sequences
413 (trimmed for >Q30) were identified by BLASTN (Altschul et al., 1990) and listed in Table
414 S1. Hydrogenase *hhyL* amino acid sequences were aligned using ClustalW (Larkin et al., 2007)
415 and phylogenetic analyses were carried out in Mega 5.2 (Tamura et al., 2011). Relationships
416 were determined using a Maximum Likelihood method based on the Whelan and Goldman
417 model (Whelan and Goldman, 2001) and checked for consistency using parsimony. The *hhyL*
418 gene from archaeon *Sulfolobus islandicus* HVE10/4 was used as an outgroup. A 100 bootstrap
419 maximum likelihood tree was constructed using Mega 5.2.

420 The gene sequences obtained for strains HFI6, HFI7, HFI8, and HFI9 were deposited in
421 GenBank under accession numbers KC661265, KC661266, KF444073, and KF444074 for the
422 16S rRNA genes and under accession numbers KC661267, KC661268, KC661269, and
423 KC661270 for the *hhyL* genes. 16S rRNA gene sequences were compared with published
424 sequences in the National Center for Biotechnology Information (NCBI) gene databases
425 (BLASTN, <http://blast.ncbi.nlm.nih.gov>) for phylogenetic identification (Table S1).

426 **H₂ uptake assays**

427 H₂ oxidation rates were determined routinely by measuring the decrease in H₂ mole
428 fractions in the microbial culture headspace over time. Microbial strains were cultivated
429 aerobically on solid (R2A) or liquid (TSB) medium inside 160 ml glass serum vials. H₂ uptake
430 rate measurements were initiated by isolating the serum vial headspace from the atmosphere with
431 a crimped stopper and vials were slightly pressurized after closure by adding 15 ml of sterile lab
432 air. Liquid cultures were continuously agitated at 200 rpm during the H₂ uptake assay to facilitate
433 gas exchange across the air-liquid interface. The change in headspace H₂ was measured three

434 times at approximately forty-minute intervals. H₂ uptake followed apparent first-order kinetics
435 over the small range (0.1 to 4 ppm) of laboratory atmospheric H₂ mole fractions: $H_2(t) =$
436 $H_2(0)e^{-bt}$. First-order rate constants were determined from the slope (-b) of the logarithmic
437 decrease in the headspace H₂ mole fraction. H₂ oxidation rates are reported at a H₂ mole fraction
438 of 530 ppb, the estimated global mean (Novelli et al., 1999).

439 H₂ mole fractions were measured using a Gas Chromatograph (GC, Model 2014,
440 Shimadzu Co., Kyoto, Japan) retrofitted with a Helium ionization Pulsed Discharge Detector
441 (HePDD, D-4-I-SH17-R Model, Valco Instruments Co. Inc., Houston, Texas). The instrument is
442 similar to a recently described system for measuring H₂ at atmospheric levels (approximately
443 530 ppb) and has an improved precision, linearity and stability compared to methods that use a
444 mercuric oxide detector (Novelli et al., 2009). Details of the instrument design and performance
445 are publically accessible in Meredith (2012). Stainless steel flasks containing compressed air
446 were used as working standards with ambient H₂ mole fractions. These were calibrated using the
447 GC-HePDD system against a tertiary standard (514.3 ppb H₂ in air, aluminum 150A tank,
448 Airgas, Radnor, PA) tied to the NOAA CMD/ESRL H₂ scale. Precisions, assessed by repeated
449 standard measurements, were typically <1% (1 sigma) on the Shimadzu GC-HePDD.

450 The precision for H₂ oxidation rate measurements is taken as two times the standard
451 deviation of measurements of the H₂ uptake in sterile control vials containing the same (liquid or
452 solid) medium as the culture vials. This precision serves as the effective detection limit, that is,
453 the minimum H₂ oxidation rate that is distinguishable from zero by the measurement. Detection
454 limits were determined separately for the time series of H₂ uptake rates measured in control vials
455 for strain HFI8 and *R. equi* because of the difference in medium, and were between (± 0.12 and

456 $\pm 0.24 \text{ nmol h}^{-1}$). H_2 uptake thresholds were determined after allowing the cultures to take up H_2
457 mole fractions for at least 90 minutes until headspace H_2 mole fractions reached stable values.

458 The Michaelis-Menten substrate affinity (K_m) describes the affinity of H_2 uptake, relevant
459 to the broad range of H_2 concentrations that occur in soils (H_2 mole fractions ranging from 0.01
460 to 1000 ppm) (Schink, 1997; Constant et al., 2008). Kinetic parameters of H_2 uptake were
461 determined in sporulated *Streptomyces* cultures and in the stationary phase cultures of *R. equi*.
462 The dependency of H_2 uptake rates on initial H_2 mole fractions were determined over a range of
463 initial headspace H_2 mole fractions (set at about eight levels between 0.5 and 35 ppm H_2 by
464 injecting a 1% H_2 in N_2 mix into the sealed headspace). Headspace H_2 was measured twice, 15
465 minutes apart in each culture containing different initial H_2 concentrations, and H_2 uptake was
466 calculated from the linear uptake rate. The K_m and the maximum reaction rate (V_{\max}) for each
467 strain was determined from Lineweaver-Burk (LB) plots of the inverse of the uptake rate ($1/V$)
468 versus the inverse of the substrate concentration ($1/S$) the initial H_2 mole fraction. K_m was
469 determined as the $K_m = -1 / x\text{-intercept}$ and V_{\max} as $V_{\max} = 1/y\text{-intercept}$ (Constant et al., 2008).
470 As a crosscheck for the quality of the reported kinetic parameters, Eadie-Hofstee (EH) plots of V
471 versus V/S were used to determine K_m from $K_m = -\text{slope}$. K_m and V_{\max} values were reported for a
472 given strain only if the LB and EH K_m values methods agreed within 50%. A typical LB and EH
473 plot is shown in Figure S7. H_2 uptake thresholds were determined after allowing the cultures to
474 take up H_2 mole fractions for at least 90 minutes until headspace H_2 mole fractions reached
475 stable values.

476 **Lifecycle analysis of *Streptomyces* spp.**

477 The life cycle of *Streptomyces* spp. cultures was tracked in parallel with the H_2 uptake to
478 test the influence of developmental stage on atmospheric H_2 uptake. Serum vials (160 mL)

479 containing 10 ml of R2A medium were inoculated with 100 μ l of the spore suspension onto the
480 agar surface. Control vials were supplemented with 100 μ l sterile H₂O. The developmental stages
481 were assessed by microscopy, using a Zeiss Axio Imager.M1 microscope and Axio Cam MRm
482 camera using Axio Vision (4.8) software (Zeiss, Peabody, MA).

483 Growth rates of filamentous organisms grown on solid media are difficult to measure;
484 instead, photographs of the fractional area covered by *Streptomyces* colonies in the serum vial
485 were used as an indication of growth rate. Final aerial biomass was quantified by a protein assay.
486 Aerial biomass was aseptically harvested using a metal spatula and transferred to 1.5 ml tubes
487 containing 0.3 g of glass beads (0.2 mm diameter) and 0.7 ml water. Cells were vortexed for 5
488 min at 2000 rpm followed by cooling on ice and then sonicated with three 30 s bursts and 1 min
489 intermittent cooling on ice. Residues of membranes and nucleic acids were removed by
490 transferring 0.5 ml of the protein extract to Costar[®] Spin-X[®] microcentrifuge filter tubes
491 (Corning, Inc., Corning, NY) and centrifuging at 10,000 rpm for 15 minutes. Protein
492 concentrations were determined using the Pierce BCA protein assay kit (Thermo Scientific,
493 Rockford, IL) and a Synergy 2 Microplate Reader (BioTek, Winooski, VT) controlled by Gen5
494 (1.04.5) software.

495 To determine whether H₂ uptake in the aerial fraction (containing hyphae and spores) of a
496 *Streptomyces* culture would continue to take up H₂ when separated from the substrate mycelium
497 and medium, H₂ uptake rates were measured before and after by gently rolling between 2.5 and
498 10 g of 4 mm glass beads (Table 2) over *Streptomyces* sp. HFI8 lawns of various ages (2-15
499 days). The lawns grew on R2A solid medium in a serum vial and the aerial biomass was
500 transferred to a sterile glass serum vial containing no medium (Figure S5). H₂ uptake rates were
501 measured in the original culture vial, the lawn was treated with the glass beads and aerial

502 biomass was transferred immediately by moving the glass beads to a sterile vial. H₂ uptake rates
503 were measured over the next 2-4 h in the sterile vial containing the isolated aerial biomass on
504 glass beads, and in the original vial containing medium and the remaining substrate mycelium.
505 The amount of biomass that was transferred was quantified using the protein assay described
506 above. This procedure was performed for six replicates at different time points after sporulation
507 and with different amounts of glass beads (Table 2, Samples 1-6). In addition, the effect of the
508 glass beads on H₂ uptake in the absence of transfer was tested in six control samples. These
509 samples were treated with the glass beads, but the beads remained in the original vials (Table 2,
510 Samples 7-12) and H₂ uptake rates were measured in the same vials before and after disruption
511 by glass beads.

512 **Growth phase analysis of *R. equi***

513 The relationship between the growth phase and H₂ uptake of *R. equi* was assessed in
514 liquid cultures. *R. equi* was inoculated by adding 100 µl of a cell suspension into 20 ml sterile
515 TSB (Bacto™ Tryptic soy broth, BD) liquid medium in 160 ml glass serum vials. All cultures
516 were incubated at 30°C and shaken at 200 rpm. Growth was monitored by measuring the optical
517 density (OD) of *R. equi* cultures as the absorbance at 600 nm at 25°C in the Synergy 2
518 Microplate Reader. The relationship between OD and protein concentration was established by
519 constructing a calibration curve between OD measurements of serial dilutions with known
520 protein concentrations. *R. equi* protein concentrations were determined using the same general
521 procedure as described for the *Streptomyces* spp. The growth phase in *R. equi* cultures were
522 established using the semilogarithmic plot of the growth curve (Figure 2), where the exponential
523 growth phase is taken as the period with the maximum, sustained positive slope. Late
524 exponential phase was defined as the time when the growth rate slowed down, as identified by a

525 decreasing slope of the growth curve. Finally, stationary phase occurred where the growth curve
526 slope was zero.

527 H_2 uptake by *R. equi* was low. A concentration/dilution experiment was performed to test
528 whether the negligible H_2 oxidation rates at low cell densities in early exponential growth phase
529 were the result of a lack of H_2 oxidation activity or the low signal-to-noise ratio due to the small
530 number of active cells. *R. equi* cultures were inoculated at the beginning of the experiment,
531 concentrated in exponential phase on day 1.9 by centrifugation at 8000 rpm for 10 min, and re-
532 suspended into either fresh TSB or in sterile H_2O to final densities of 160 and 110- $\mu\text{g protein ml}^{-1}$
533 1 in TSB and H_2O , respectively. This was within the range of densities observed in late
534 exponential and stationary phases (100-230 $\mu\text{g protein ml}^{-1}$). Additionally, a sample was taken
535 on day 7.8 in stationary phase (at a density of 190 $\mu\text{g protein ml}^{-1}$) and was diluted in TSB or
536 sterile H_2O to cellular densities of 45 and 38 $\mu\text{g protein ml}^{-1}$ respectively, to match the density in
537 the early exponential phase (10-100 $\mu\text{g protein ml}^{-1}$). For both the concentration and dilution
538 experiments, the cell pellets resulting from centrifugation were not washed during the procedure
539 so that some extracellular material and original culture medium (< 1 ml) was diluted into fresh
540 TSB or H_2O to a maximum final concentration of 1/5th. H_2 uptake rates in the headspace of the
541 concentrated or diluted samples were measured as described above.

542 **Acknowledgements**

543 The authors are grateful to Paula Welander for advice in the lab and to Diane Ivy for
544 assistance with measurements. Strain *Streptomyces griseoflavus* Tu4000 was kindly contributed
545 to this study by genome authors Michael Fischbach and John Clardy via Joshua Blodgett. L.K.M.
546 is grateful for the opportunity to attend the MBL Microbial Diversity Course. L.K.M. was
547 supported by from the following funding sources: NSF Graduate Research Fellowship, multiple

548 grants from NASA to MIT for the Advanced Global Atmospheric Gases Experiment (AGAGE),
549 MIT Center for Global Change Science, MIT Joint Program on the Science and Policy of Global
550 Change, MIT Martin Family Society of Fellows for Sustainability, MIT Ally of Nature Research
551 Fund, MIT William Otis Crosby Lectureship, and MIT Warren Klein Fund. D. R. was funded
552 through MIT Undergraduate Research Opportunities Program (UROP) with support from the
553 Lord Foundation and Jordan J. Baruch Fund (1947) and was supported by the Harvard Forest
554 REU Program.

555

556 **Conflict of Interest**

557 Authors and co-authors have no conflicts of interest to declare.

558

559 **References**

560 Allen, A. (1995) Soil science and survey at Harvard Forest. *Soil Surv Horiz* 36

561 Altschul,S.F., Gish W., Miller, W., Myers, E.W., Lipman, D.J. (1990) Basic Local Alignment
562 Search Tool. *J Mol Biol* 215: 403–410.

563 Bergey, D.H. and Gibbons, N.E. (1957) *Bergey’s manual of determinative bacteriology*, 7th
564 edn. Baltimore, USA: Williams & Wilkins Company.

565 Berney, M. and Cook, G.M. (2010) Unique flexibility in energy metabolism allows
566 *mycobacteria* to combat starvation and hypoxia. *PloS ONE* 5: e8614.

567 Conrad, R and Seiler, W. (1981) Decomposition of atmospheric hydrogen by soil
568 microorganisms and soil enzymes. *Soil Biol Biochem* 13: 43–49.

- 569 Conrad, R. and Seiler, W. (1985) Influence of temperature, moisture, and organic carbon on the
570 flux of H₂ and CO between soil and atmosphere: field studies in subtropical regions. J
571 Geophys Res 90: 5699–5709.
- 572 Conrad, R., Aragno, M., and Seiler, W. (1983a) Production and consumption of hydrogen in a
573 eutrophic lake. Appl Environ Microbiol 45: 502-510.
- 574 Conrad, R., Aragno, M., and Seiler, W. (1983b) The inability of hydrogen bacteria to utilize
575 atmospheric hydrogen is due to threshold and affinity for hydrogen. FEMS Microbiol
576 Lett 18: 207–210.
- 577 Conrad, R. (1996) Soil microorganisms as controllers of atmospheric trace gases (H₂, CO, CH₄,
578 OCS, N₂O, and NO). Microbiol Rev 60: 609–640.
- 579 Conrad, R. (1999) Soil microorganisms oxidizing atmospheric trace gases (CH₄, CO, H₂, NO).
580 Ind J Microbiol 39: 193–203.
- 581 Constant, P., Poissant, L., and Villemur, R. (2008) Isolation of *Streptomyces* sp. PCB7, the first
582 microorganism demonstrating high-affinity uptake of tropospheric H₂. ISME J 2: 1066–
583 1076.
- 584 Constant, P., Poissant, L., and Villemur, R. (2009) Tropospheric H₂ budget and the response of
585 its soil uptake under the changing environment. Sci Total Environ 407: 1809–1823.
- 586 Constant, P., Chowdhury, S.P., Pratscher, J., and Conrad, R. (2010) *Streptomyces* contributing
587 to atmospheric molecular hydrogen soil uptake are widespread and encode a putative
588 high-affinity [NiFe]-hydrogenase. Env Microbiol 12: 821–829.
- 589 Constant, P., Chowdhury, S.P., Hesse, L., and Conrad, R. (2011a) Co-localization of atmospheric
590 H₂ oxidation activity and high affinity H₂-oxidizing bacteria in non-axenic soil and sterile
591 soil amended with *Streptomyces* sp. PCB7. Soil Biol Biochem 43: 1888–1893.

- 592 Constant, P., Chowdhury, S.P., Hesse, L., Pratscher, J., and Conrad, R. (2011b) Genome data
593 mining and soil survey for the novel group 5 [NiFe]-hydrogenase to explore the diversity
594 and ecological importance of presumptive high affinity H₂-oxidizing bacteria. *Appl*
595 *Environ Microb* 77: 6027–6035.
- 596 Ehhalt, D.H. and Rohrer, F. (2009) The tropospheric cycle of H₂: a critical review. *Tellus B* 61:
597 500–535.
- 598 El-Nakeeb, M.A. and Lechevalier, H.A. (1963) Selective isolation of aerobic Actinomycetes.
599 *Appl Microbiol* 11: 75–77.
- 600 Flårdh, K. and Buttner, M.J. (2009) *Streptomyces* morphogenetics: dissecting differentiation in a
601 filamentous bacterium. *Nat Rev Microbiol* 7: 36–49.
- 602 Guo, R. and Conrad, R. (2008) Extraction and characterization of soil hydrogenases oxidizing
603 atmospheric hydrogen. *Soil Biol Biochem* 40: 1149–1154.
- 604 Häring, V. and Conrad, R. (1994) Demonstration of two different H₂-oxidizing activities in soil
605 using an H₂ consumption and a tritium exchange assay. *Biol Fert Soils* 17: 125–128.
- 606 Hardisson, C., Manzanal, M.B., Salas, J.A., and Suarez, J.E. (1978) Fine structure, physiology
607 and biochemistry of arthrospore germination in *Streptomyces antibioticus*. *J. Gen.*
608 *Microbiol.* 105: 203–214.
- 609 Hirsch, C.F. and Ensign, J.C. (1976) Nutritionally defined conditions for germination of
610 *Streptomyces viridochromogenes* spores. *J. Bacteriol.* 126: 13–23.
- 611 Kieser, T., Bibb, M.J., Buttner, M.J., Chater, K.F., and Hopwood, D.A. (2000) Practical
612 *Streptomyces* genetics. Norwich, UK: John Innes Foundation.
- 613 King, G.M. (2003a) Contributions of atmospheric CO and hydrogen uptake to microbial
614 dynamics on recent Hawaiian volcanic deposits. *Appl Environ Microb* 69: 4067–4075.

- 615 King, G.M. (2003b) Uptake of carbon monoxide and hydrogen at environmentally relevant
616 concentrations by mycobacteria. *Appl Env Microbiol* 69: 7266–7272.
- 617 Lane DJ (1991) 16S/23S rRNA sequencing. In *Nucleic acid techniques in bacterial systematics*.
618 Stackebrandt, E. and Goodfellow, M. (eds). John Wiley and Sons, New York, pp. 115-
619 148.
- 620 Larkin, M. A., Blackshields, G., Brown, N. P., Chenna, R., McGettigan, P. A., McWilliam, H.,
621 Valentin, F., Wallace, I. M., Wilm, A., Lopez, R., Thompson, J.D., Gibson, T.J., and
622 Higgins, D. G. (2007) Clustal W and Clustal X version 2.0. *Bioinformatics* (Oxford,
623 England) 23: 2947–8.
- 624 Madsen, E.L. (2005) Identifying microorganisms responsible for ecologically significant
625 biogeochemical processes. *Nat Rev Micro* 3: 439–446.
- 626 Meredith, L.K. (2012) Field Measurement of the Fate of Atmospheric H₂ in a Forest
627 Environment: from Canopy to Soil. Doctor of philosophy thesis, Massachusetts Institute
628 of Technology, MIT Center for Global Change Science, 250 pp.
629 (<http://globalchange.mit.edu/research/publications/2366>)
- 630 Miguélez, E.M., Hardisson, C., and Manzanal, M. (1999) Hyphal death during colony
631 development in *Streptomyces antibioticus*: morphological evidence for the existence of a
632 process of cell deletion in a multicellular prokaryote. *J Cell Biol* 145: 515–525.
- 633 Novelli, P.C., Lang, P.M., Masarie, K.A., Hurst, D.F., Myers, R., Elkins, J.W. (1999) Molecular
634 hydrogen in the troposphere: Global distribution and budget. *J Geophys Res* 104: 30,427–
635 30,444.

- 636 Novelli, P.C., Crotwell, A.M., and Hall, B.D. (2009) Application of gas chromatography with a
637 pulsed discharge helium ionization detector for measurements of molecular hydrogen in
638 the atmosphere. *Environ Sci Technol* 43: 2431–2436.
- 639 Porter, J.N., Wilhelm, J.J., and Tresner, H.D. (1960) Method for the preferential isolation of
640 Actinomycetes from soils. *Appl Microbiol* 8: 174-178.
- 641 Prescott, J.F. (1991) *Rhodococcus equi*: an animal and human pathogen. *Clin Microbiol Rev* 4:
642 20–34.
- 643 Rahn, T., Eiler, J. M., Kitchen, N., Fessenden, J. E., and Randerson, J. T. (2002) Concentration
644 and δD of molecular hydrogen in boreal forests: Ecosystem-scale systematics of
645 atmospheric H₂. *Geophys Res Lett* 29: 1–4.
- 646 Scherr, N. and Nguyen, L. (2009) *Mycobacterium* versus *Streptomyces* - we are different, we are
647 the same. *Curr Opin Microbiol* 12: 699–707.
- 648 Schink, B. (1997) Energetics of syntrophic cooperation in methanogenic degradation. *Microbiol*
649 *Mol Biol Rev* 61: 262-280.
- 650 Schrempf, H. (2008) Streptomycetaceae: life style, genome, metabolism and habitats.
651 *Encyclopedia of Life Sciences*. Chichester, UK: John Wiley & Sons, pp 1–7.
- 652 Schuler, S. and Conrad, R. (1990) Soils contain two different activities for oxidation of
653 hydrogen. *FEMS Microbiol Ecol* 73: 77–83.
- 654 Smeulders, M.J., Keer, J., Speight, R.A., and Williams, H.D. (1999) Adaptation of
655 *Mycobacterium smegmatis* to stationary phase. *J Bacteriol* 181: 270-283.
- 656 Smith-Downey, N.V., Randerson, J.T., and Eiler, J.M. (2008) Molecular hydrogen uptake by
657 soils in forest, desert, and marsh ecosystems in California. *J Geophys Res* 113: 1–11.

- 658 Straight, P.D. and Kolter, R. (2009) Interspecies chemical communication in bacterial
659 development. *Ann Rev Microbiol* 63: 99–118.
- 660 Szabó, G. and Vitalis, S. (1992) Sporulation without aerial mycelium formation on agar medium
661 by *Streptomyces bikiniensis* HH1, an A-factor-deficient mutant. *Microbiol.* 138: 1887–
662 1892.
- 663 Tamura, K., Peterson, D., Peterson, N., Stecher, G., Nei, M., and Kumar, S. (2011) MEGA5:
664 molecular evolutionary genetics analysis using maximum likelihood, evolutionary
665 distance, and maximum parsimony methods. *Mol Biol Evol* 28: 2731–9.
- 666 Ueda, K., Kawai, S., Ogawa, H., Kiyama, A., Kubota, T., Kawanobe, H., and Beppu, T. (2000)
667 Wide distribution of interspecific stimulatory events on antibiotic production and
668 sporulation among *Streptomyces* species. *J Antibiot* 53: 979–982.
- 669 Whelan, S. and Goldman, N. (2001) A general empirical model of protein evolution derived
670 from multiple protein families using a maximum-likelihood approach. *Mol Biol* 18: 691–
671 9.
- 672 Xiao, X., Prinn, R.G., Simmonds, P.G., Steele, L.P., Novelli, P.C., Huang, J., Langenfelds, R.L.,
673 O’Doherty, S., Krummel, P.B., Fraser, P.J., Porter, L.W., Weiss, R.F., Salameh, P. and
674 Wang, R.H.J. (2007) Optimal estimation of the soil uptake rate of molecular hydrogen
675 from AGAGE and other measurements, *J Geophys Res*, 112: 1-15.
- 676 Yonemura, S., Yokozawa, M., Kawashima, S., and Tsuruta, H. (2000) Model analysis of the
677 influence of gas diffusivity in soil on CO and H₂ uptake. *Tellus B* 52: 919–933.

678

679 **Table and Figure Legends**

680 Table 1. H₂ oxidation rates weighted by biomass (final protein mass) for Harvard Forest
681 Isolate (HFI) strains and strains from culture collections (*S. cattleya*, *S. griseoflavus*, *R. equi*) at
682 typical atmospheric (~0.53 ppm) H₂ mole fractions. H₂ uptake affinity (K_m), the maximum
683 reaction rate (V_{max}), and the minimum threshold for consumption are listed for each culture.

684

685 Table 2. Effect of physical disturbances of the aerial structure on H₂ oxidation rates in
686 sporulated cultures of *Streptomyces* sp. HFI8. Gently rolling 4 mm diameter glass beads over
687 culture lawns (Figure S5) reduced the observed H₂ uptake. The H₂ oxidation rates (the 5th
688 column) in twelve whole cultures of strain HFI8 growing in serum vials on solid R2A medium
689 were measured between 2 and 15 days after inoculation (the 2nd column). In samples 1-6, the
690 aerial biomass was isolated from substrate biomass using glass beads to transfer aerial biomass to
691 an empty, sterile vial. The amount of transferred biomass was measured by protein assay (the 4th
692 column). We tested using different amounts (2.5 and 10g) of 4 mm diameter glass beads (the 3rd
693 column). H₂ uptake is reported for the fraction of aerial biomass transferred to glass beads (the
694 6th column) and for the fraction of the lawn remaining in the original vial in the medium (the 7th
695 column) measured within 2-4 hours. In samples 7-12, all biomass was left in the original vial,
696 and H₂ oxidation rates were measured before and after treatment with glass beads. The difference
697 in uptake due to the procedure (the sum of the uptake rates reported in the 6th and the 7th column
698 minus the uptake before transfer in the 5nd column) is reported in the 8th column.

699

700 Figure 1. High-resolution time series of H₂ uptake in three replicate cultures of
701 *Streptomyces* sp. HFI8. The lettered arrows at various time points correspond to the micrographs
702 of the life cycle shown in Figure S4: (A) the substrate mycelium, (B) the formation of aerial

703 hyphae and onset of sporulation, (C-H) cultures contain mainly spores. Enlarged inset shows the
704 higher resolution measurements taken during the first four days. The detection limit (dashed
705 lines) of $\pm 0.24 \text{ nmol h}^{-1}$ is reported as the double standard deviation of four values measured in
706 uninoculated control vials (black dots).

707

708 Figure 2. Consumption of H_2 by *Rhodococcus equi* in liquid culture. (a) H_2 oxidation
709 rate, (b) cell biomass (protein concentration). All data are shown for three liquid culture
710 replicates. The detection limit (dashed lines) is of $\pm 0.12 \text{ nmol h}^{-1}$ and calculated as the double
711 standard deviation of ten values measured in uninoculated control vials (black dots). Colored
712 triangles show the results of concentration and dilution experiments. Cells in exponential phase
713 were concentrated in either fresh TSB medium (green) or water (orange) to match protein
714 concentrations in late exponential and stationary phase. Alternatively, cells from stationary phase
715 were diluted in either fresh TSB medium (green) or water (orange) to protein concentrations
716 similar to those in exponential phase cultures.

717

718 Table S1. The top database matches for strain HFI6 - HFI9 16S rRNA gene and *hhyL*
719 nucleotide sequences indicate that the strains are *Streptomyces* spp. containing *hhyL* sequences.
720 The GenBank accession number is listed for each deposited sequence. The results of NCBI
721 Megablast BLAST search are listed for each sequence, where queries were made for the 16S
722 rRNA sequences against the 16S rRNA gene sequence database and for the *hhyL* sequences
723 against the entire nucleotide sequence database. The top match for each BLAST search is listed
724 along with the total score, E value, and maximum identity of the match. Strain HFI6 - HFI9 16S
725 rRNA gene sequences were 100% identical to several different strains of *Streptomyces* spp.

726 Strain HFI6 - HFI9 *hhyL* sequences are highly similar to published cultured and uncultured *hhyL*
727 sequences, of which some were submitted to public databases as *hydB*-like genes, though the
728 *hhyL* terminology has been more recently adopted (Constant et al., 2011b).

729

730 Figure S1. Photographs of *Streptomyces griseoflavus* Tu4000 and *Streptomyces* sp. HFI6
731 - HFI9 soil isolate colonies on R2A medium plates. *S. griseoflavus* Tu4000 had the smooth and
732 waxy appearance of a *bld* (bald) *Streptomyces* mutant, while strains HFI6 - HFI9 formed fuzzy
733 colonies consistent with the presence of aerial hyphae. The pigmentation of strains HFI6 - HFI8
734 was light pink and strain HFI9 was darker with a brown exudate secreted into the surrounding
735 medium. HFI6 - HFI9 strains had the strong scent of geosmin, while *S. griseoflavus* Tu4000 did
736 not.

737

738

739 Figure S2. Photomicrographs of *Streptomyces griseoflavus* Tu4000 and *Streptomyces* sp.
740 HFI6 - HFI9 soil isolate cultures on R2A medium plates. The same samples are photographed in
741 Figure S1. Only substrate mycelia are visible in the *S. griseoflavus* Tu4000 colony, while HFI6 -
742 HFI9 strains had plentiful aerial hyphae.

743

744 Figure S3. Molecular phylogenetic analysis of *hhyL* sequences by the Maximum
745 Likelihood method. The diversity of the high-affinity group 5 [NiFe]-hydrogenase (*hhyL*)
746 sequences of the strains (bold) we tested for H₂ uptake (Table 1) are compared with *hhyL*
747 sequences from the NCBI microbial genome database in this amino acid tree. The *hhyL*-
748 containing *Streptomyces* sequences form two distinct clusters at a deep 99% bootstrap branch:

749 Cluster 1 and Cluster 2. Isolates that have been tested for H₂ uptake are marked to indicate
750 whether (*) or not (†) high-affinity H₂ uptake was observed. Culture collection strains
751 investigated in this study were selected to broaden representation across the clusters and genera:
752 *Streptomyces griseoflavus* Tu4000 (Cluster 1), *Rhodococcus equi* (*Actinobacterium*, Cluster 1),
753 and *Streptomyces cattleya* (Cluster 2). Strains HFI6, HFI7, HFI8, and *S. griseoflavus* Tu4000
754 *hhyL* are closely related to Cluster 1 *Streptomyces* spp. soil isolates that take up H₂ (summarized
755 in Constant et al., 2011b), while strain HFI9 *hhyL* is more closely related to the *R. equi hhyL*.
756 Cluster 2 *S. cattleya hhyL* is closely related to *Streptomyces* sp. AP1 *hhyL*, which also consumes
757 H₂ (Constant et al., 2011b). Other culture collection strains that have been tested for H₂ uptake
758 include *Ralstonia eutropha* H16 (Conrad et al., 1983b) and *Mycobacterium smegmatis* (King,
759 2003). The evolutionary history was inferred by using the Maximum Likelihood method based
760 on the Whelan and Goldman, 2010 model. The *hhyL* gene from an archaeon *Sulfolobus*
761 *islandicus* HVE10/4 was used as the outgroup. The bootstrap values are shown next to the
762 branches. Initial tree(s) for the heuristic search were obtained automatically by applying
763 Neighbor-Join and BioNJ algorithms to a matrix of pairwise distances estimated using a WAG
764 model, and then selecting the topology with superior log likelihood value. A discrete Gamma
765 distribution was used to model evolutionary rate differences among sites (5 categories (+G,
766 parameter = 1.2590)). The tree is drawn to scale, with branch lengths measured in the number of
767 substitutions per site. The analysis involved 58 amino acid sequences. There were a total of 427
768 positions in the final dataset. Evolutionary analyses were conducted in MEGA5 (Tamura et al.,
769 2011).
770

771 Figure S4. Microscopic observations of the development of *Streptomyces* sp. HFI8 show
772 that strain HFI8 underwent the full lifecycle from spore to spore in less than 1.8 days, after
773 which nearly all the viable cells existed as spores. Each panel shows a representative micrograph
774 of the culture taken on a different day after the inoculation. Image A shows the substrate
775 mycelium that grows after the germination of inoculated spores. By day 1.8 (B), septated aerial
776 hyphae (punctuated tubular branches) and fully formed spores (round cells) are present. Mainly
777 spores are present from day 2.9 to 22 (C-H) and the same persists until day 44 (not shown).
778

779 Figure S5. Photograph of serum vials during the aerial biomass removal experiments
780 (Table 2, Samples 1-6) illustrates the separation of the aerial hyphae and spores from the
781 substrate mycelium: a) vial containing an *whole* intact strain HFI8 culture (Table 2, column 5);
782 b) vial from which the aerial biomass had been isolated using glass beads leaving behind the
783 remaining *substrate* mycelium (Table 2, column 7); and c) vial containing the isolated *aerial*
784 biomass on the surface of the glass beads (Table 2, column 6). In some samples, glass beads
785 were rolled on the whole colony surface (a) and were left in the same vial with no biomass
786 transfer (Table 2, Samples 7-12).
787

788 Figure S6. Scatter plot of the initial H₂ oxidation rate versus the reduction in H₂ uptake
789 by *Streptomyces* sp. HFI8 during the glass bead procedure (Table 2; 5th and 8th columns). The
790 larger the initial H₂ oxidation rate, the larger percentage reduction by the glass beads ($R^2=0.93$),
791 regardless of culture age or the amount of glass beads used for transfer.
792

793 Figure S7: Determination of H₂ uptake kinetic parameters by the Lineweaver-Burk (LB)
794 and Eadie-Hofstee (EH) methods for *Streptomyces* sp. HFI8. The H₂ uptake rate (V) nmol h⁻¹
795 and initial H₂ concentration (S) in ppm are used to generate the LB plot as 1/V versus 1/S and
796 EH as V versus V/S. K_m was determined from the LB plot as the K_m = -1 / x-intercept (38 ppm)
797 and V_{max} as V_{max} = 1/y-intercept (30 μmol min⁻¹ g⁻¹). K_m was determined from the EH plot as K_m
798 = -slope (22 ppm). K_m and V_{max} values were reported for a given strain only if the LB and EH
799 K_m values methods agreed within 50%`
800

Table 1. H₂ oxidation rates weighted by biomass (final protein mass) for Harvard Forest Isolate (HFI) strains and strains from culture collections (*S. cattleya*, *S. griseoflavus*, *R. equi*) at typical atmospheric (~0.53 ppm) H₂ mole fractions. H₂ uptake affinity (K_m), the maximum reaction rate (V_{max}), and the minimum threshold for consumption are listed for each culture.

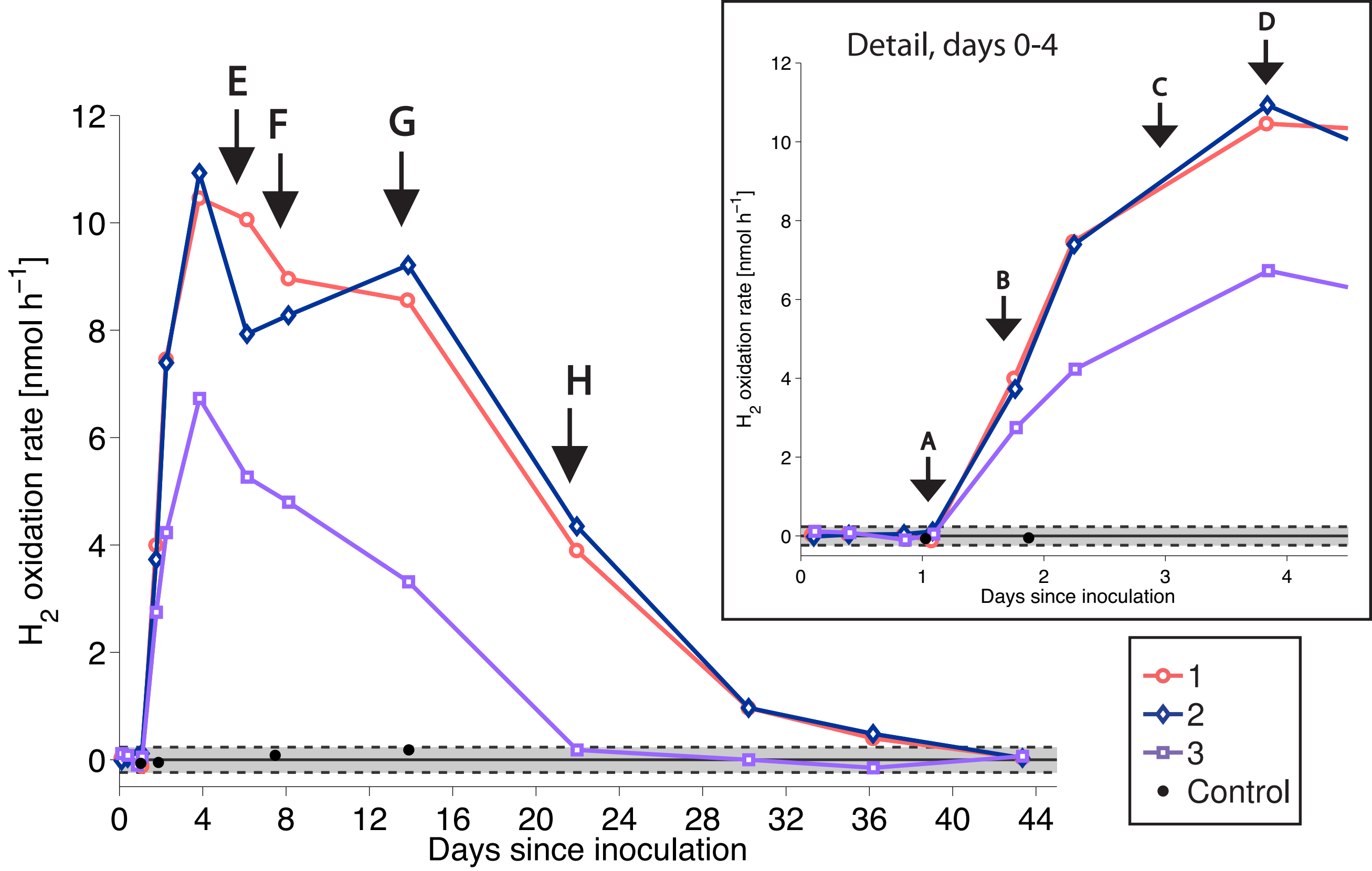
Strain	H ₂ oxidation rate [nmol min ⁻¹ g ⁻¹]	K _m * [ppm]	V _{max} * [μmol min ⁻¹ g ⁻¹]	Threshold [ppm]
<i>Streptomyces</i> sp. HFI6	780	80	180	<0.15
<i>Streptomyces</i> sp. HFI7	420	60	78	<0.12
<i>Streptomyces</i> sp. HFI8	240	40	30	<0.15
<i>Streptomyces</i> sp. HFI9	100	40	14	<0.12
<i>Streptomyces griseoflavus</i> Tu4000	0	-	-	-
<i>Streptomyces cattleya</i>	130	**	**	<0.45
<i>Rhodococcus equi</i>	10	**	**	<0.30

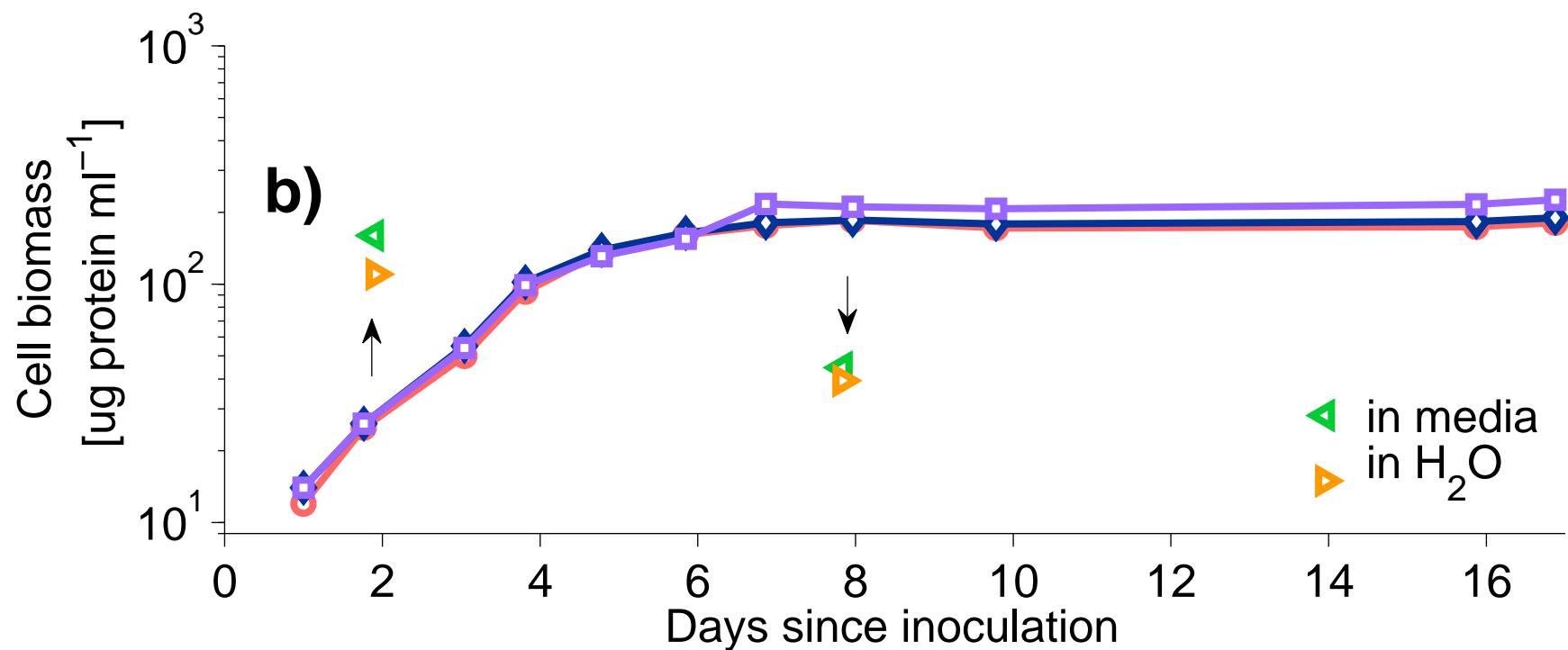
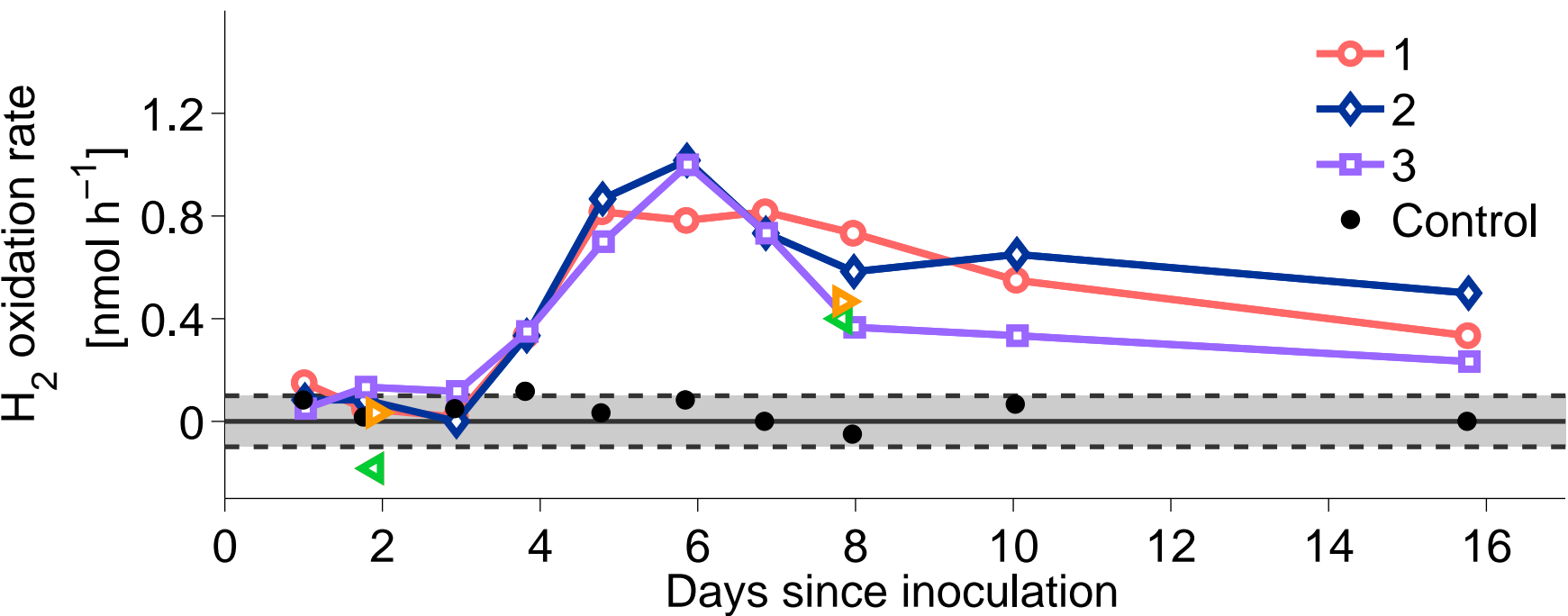
* Determined by the Lineweaver-Burke method over a 0-35 ppm H₂ range, which is less precise than the non-inverse approach, but avoids interference by low-affinity hydrogenases.

** Kinetic parameters determination did not pass quality check (Experimental Procedures).

Table 2. Effect of physical disturbances of the aerial structure on H₂ oxidation rates in sporulated cultures of *Streptomyces* sp. HFI8. Gently rolling 4 mm diameter glass beads over culture lawns (Figure S5) reduced the observed H₂ uptake. The H₂ oxidation rates (the 5th column) in twelve whole cultures of strain HFI8 growing in serum vials on solid R2A medium were measured between 2 and 15 days after inoculation (the 2nd column). In samples 1-6, the aerial biomass was isolated from substrate biomass using glass beads to transfer aerial biomass to an empty, sterile vial. The amount of transferred biomass was measured by protein assay (the 4th column). We tested using different amounts (2.5 and 10g) of 4 mm diameter glass beads (the 3rd column). H₂ uptake is reported for the fraction of aerial biomass transferred to glass beads (the 6th column) and for the fraction of the lawn remaining in the original vial in the medium (the 7th column) measured within 2-4 hours. In samples 7-12, all biomass was left in the original vial, and H₂ oxidation rates were measured before and after treatment with glass beads. The difference in uptake due to the procedure (the sum of the uptake rates reported in the 6th and the 7th column minus the uptake before transfer in the 5nd column) is reported in the 8th column.

ID	Day	Beads [g]	Aerial biomass [mg]	H ₂ oxidation rate [nmol h ⁻¹]			
				Whole	Aerial + glass beads	Substrate	Change in net uptake (%)
1	2	10	na	4.1	0.6	1.5	-1.9 (-48%)
2	8	10	0.3	6.8	0.3	2.9	-3.6 (-52%)
3	15	10	0.1	6.9	0.3	1.7	-4.9 (-71%)
4	9	2.5	1.5	3.6	0.1	2.1	-1.4 (-40%)
5	9	5	0.6	3.8	0.1	2.2	-1.4 (-37%)
6	9	10	1.1	3.8	0.1	2.1	-1.6 (-43%)
				Whole	Whole + glass beads		
7	9	10	na	2.2	1.3		-0.9 (-41%)
8	9	10	na	2.8	2.1		-0.7 (-25%)
9	9	10	na	2.4	1.5		-0.9 (-38%)
10	9	10	na	1.5	2.0		-0.3 (-20%)
11	9	10	na	2.4	2.0		-0.4 (-18%)
12	9	10	na	2.2	1.9		-0.3 (-13%)

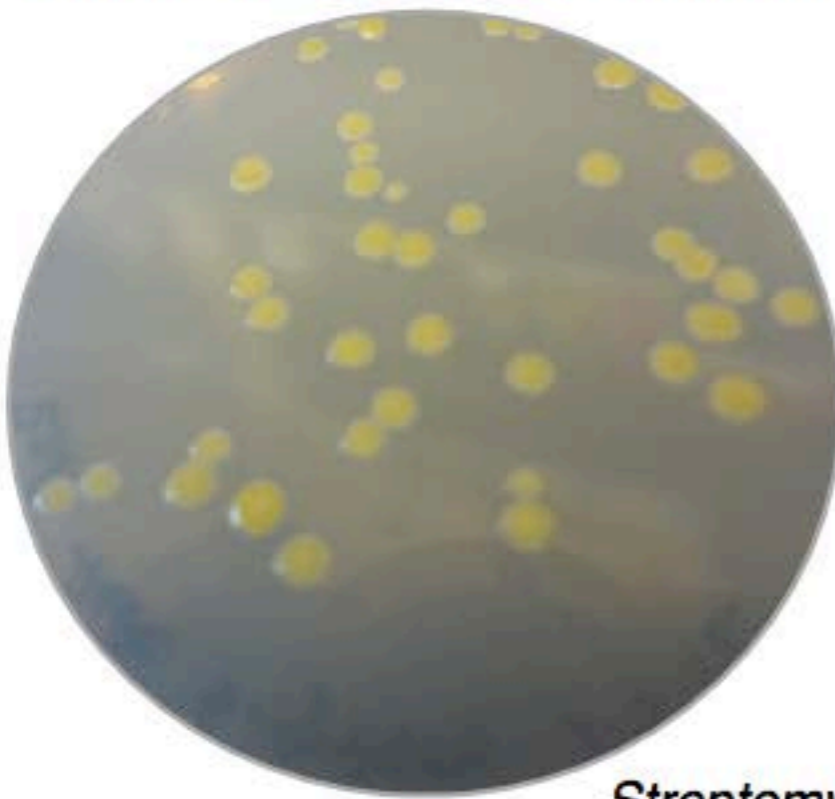




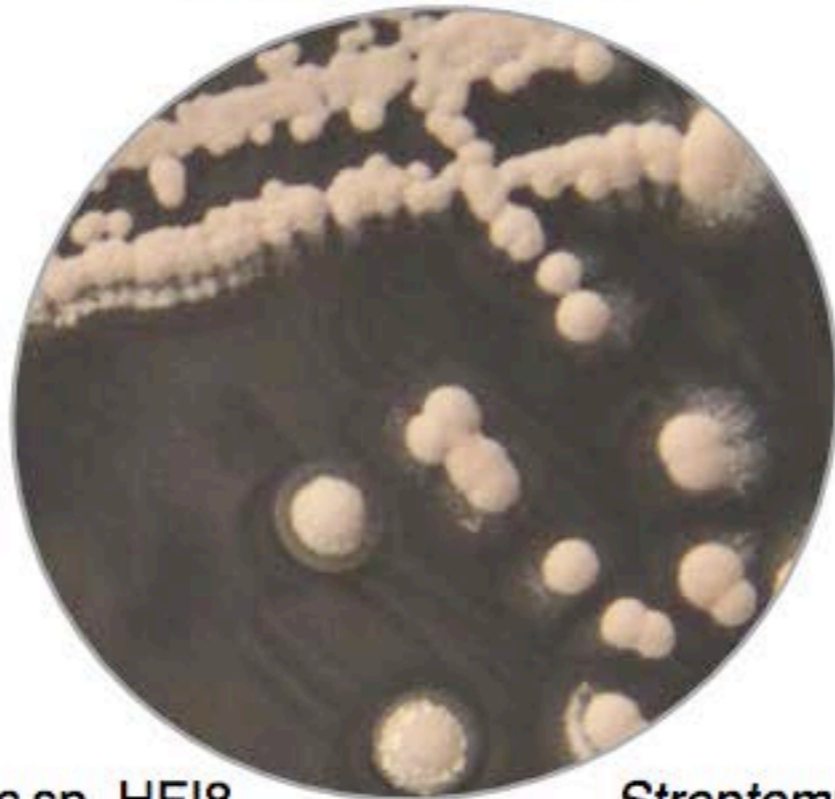
1 Table S1. The top database matches for strain HFI6 - HFI9 16S rRNA gene and *hhyL* nucleotide sequences indicate that the strains are
2 *Streptomyces* spp. containing *hhyL* sequences. The GenBank accession number is listed for each deposited sequence. The results of
3 NCBI Megablast BLAST search are listed for each sequence, where queries were made for the 16S rRNA sequences against the 16S
4 rRNA gene sequence database and for the *hhyL* sequences against the entire nucleotide sequence database. The top match for each
5 BLAST search is listed along with the total score, E value, and maximum identity of the match. Strain HFI6 - HFI9 16S rRNA gene
6 sequences were 100% identical to several different strains of *Streptomyces* spp. Strain HFI6 - HFI9 *hhyL* sequences are highly similar
7 to published cultured and uncultured *hhyL* sequences, of which some were submitted to public databases as *hydB*-like genes, though
8 the *hhyL* terminology has been more recently adopted (Constant et al., 2011b).
9

Strain	Gene	Nucleotide sequence	BLAST results				
			Accession number	Top database match (accession number)	Total Score	E value	Max ident
HFI6	16S rRNA	KC661265		<i>Streptomyces lavendulae</i> subsp. <i>lavendulae</i> strain NBRC 12344 (AB184081.2)	2532	0.0	100%
HFI7	16S rRNA	KC661266		<i>Streptomyces roseochromogenus</i> strain MJM9261 (GU296744.1)	2532	0.0	100%
HFI8	16S rRNA	KF444073		<i>Streptomyces roseochromogenus</i> strain MJM9261 (GU296744.1)	2532	0.0	100%
HFI9	16S rRNA	KF444074		<i>Streptomyces sanglieri</i> strain NBRC 100784 (NR_041417.1)	2521	0.0	100%
HFI6	<i>hhyL</i>	KC661267		<i>Streptomyces</i> sp. MP1 NiFe-hydrogenase large subunit (<i>hydB</i>) gene (GQ867040.1)	1838	0.0	95%
HFI7	<i>hhyL</i>	KC661268		<i>Streptomyces</i> sp. MP1 NiFe-hydrogenase large subunit (<i>hydB</i>) gene (GQ867040.1)	1866	0.0	96%
HFI8	<i>hhyL</i>	KC661269		<i>Streptomyces</i> sp. MP1 NiFe-hydrogenase large subunit (<i>hydB</i>) gene (GQ867040.1)	1432	0.0	97%
HFI9	<i>hhyL</i>	KC661270		<i>Streptomyces</i> sp. S9n30 partial <i>hhyL</i> gene for [NiFe]-hydrogenase (HF677116.1)	2207	0.0	99%

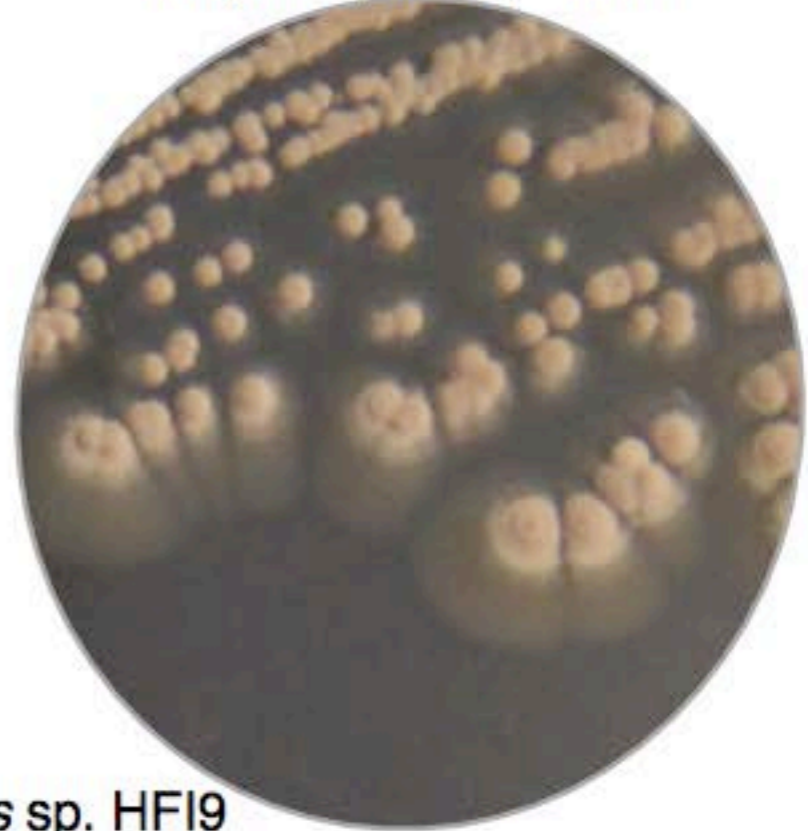
Streptomyces griseoflavus Tu4000



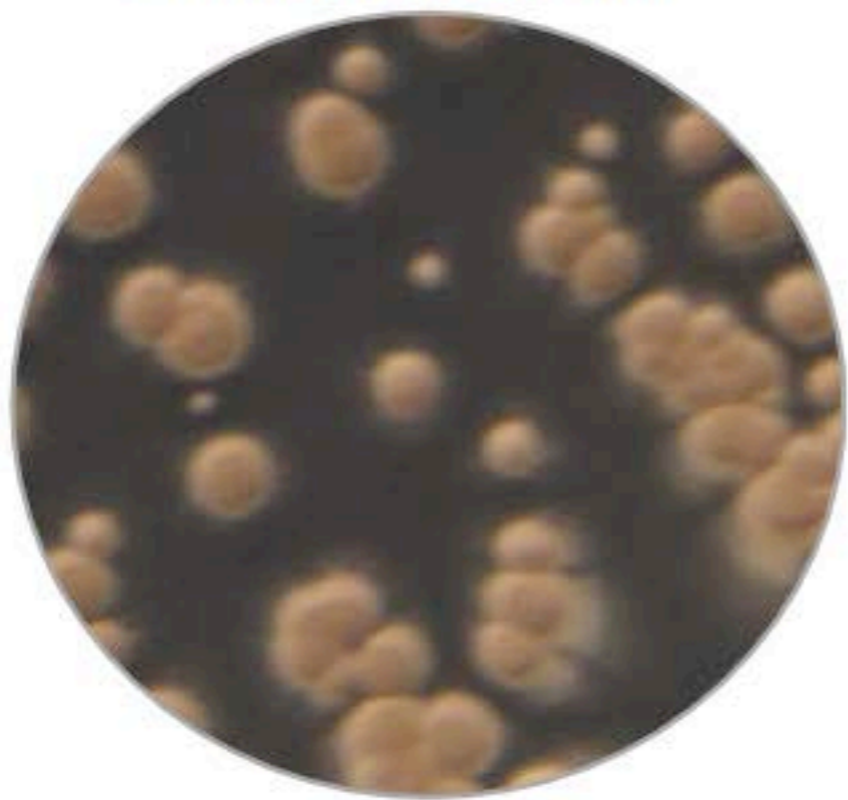
Streptomyces sp. HF16



Streptomyces sp. HF17



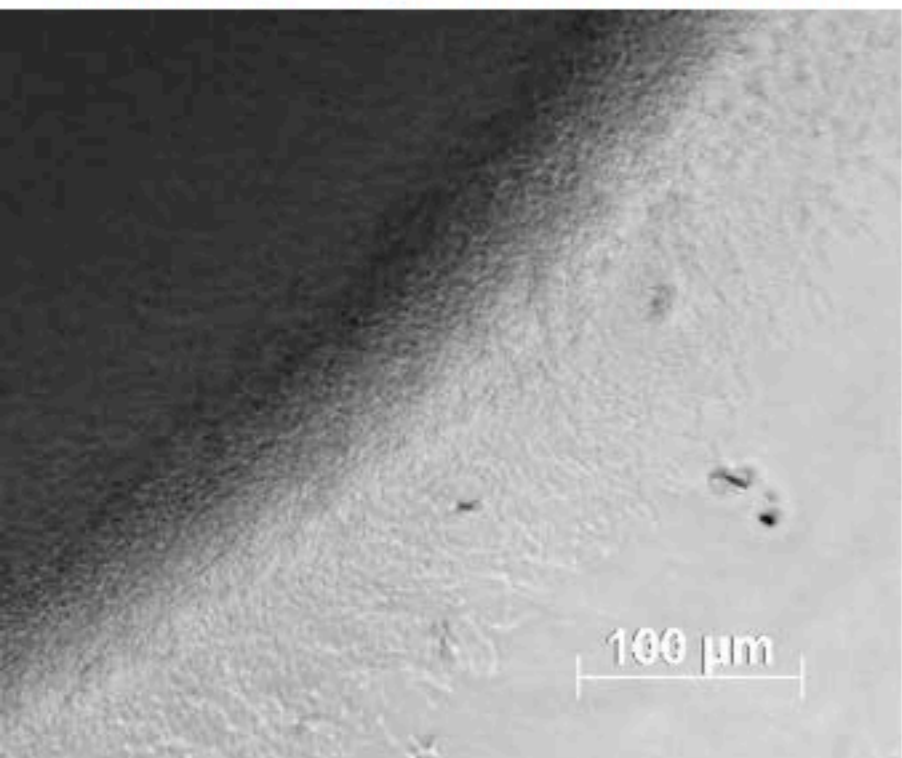
Streptomyces sp. HF18



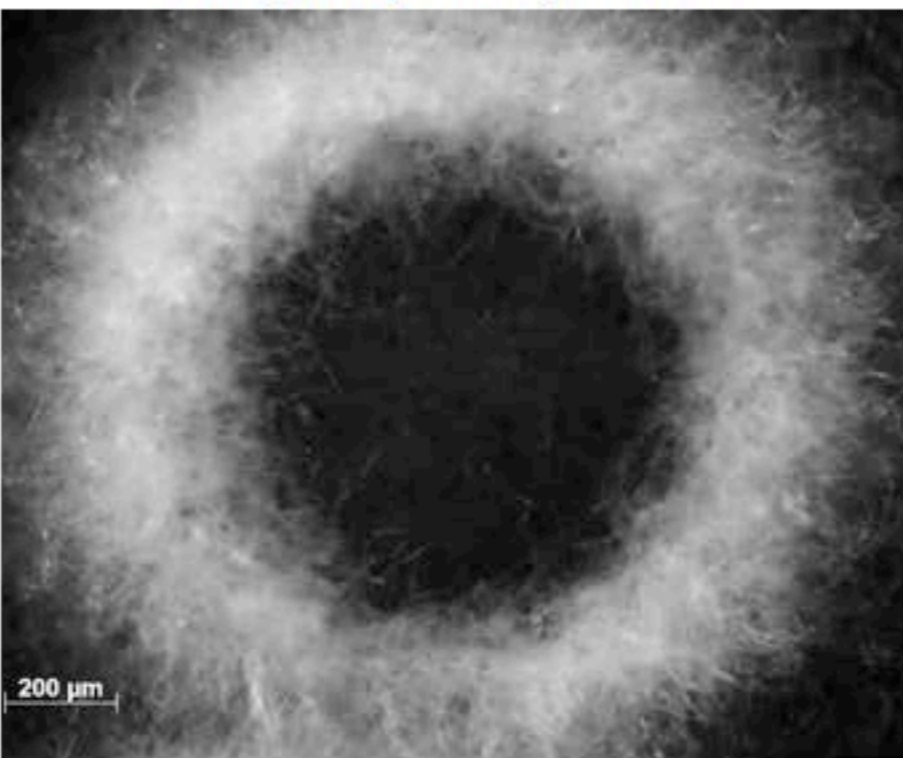
Streptomyces sp. HF19



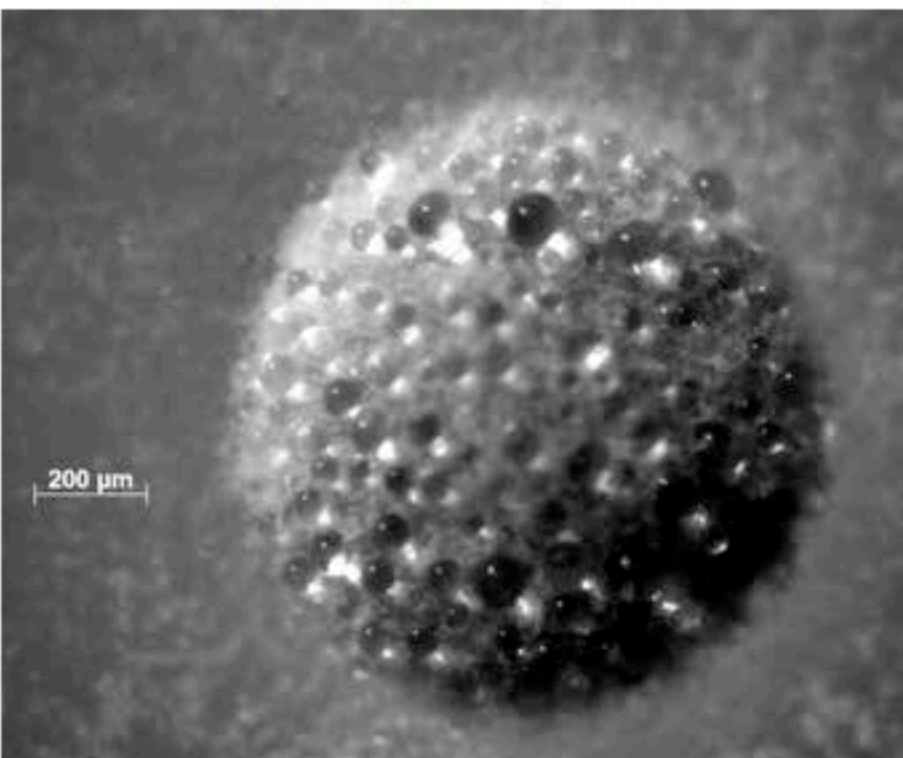
Streptomyces griseoflavus Tu4000



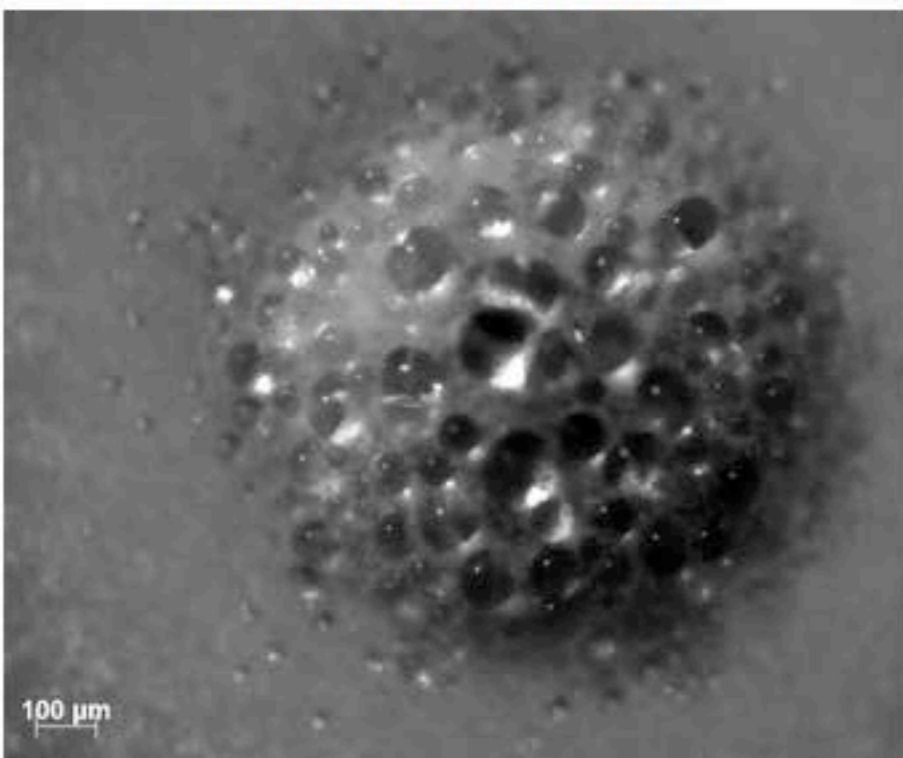
Streptomyces sp. HF16



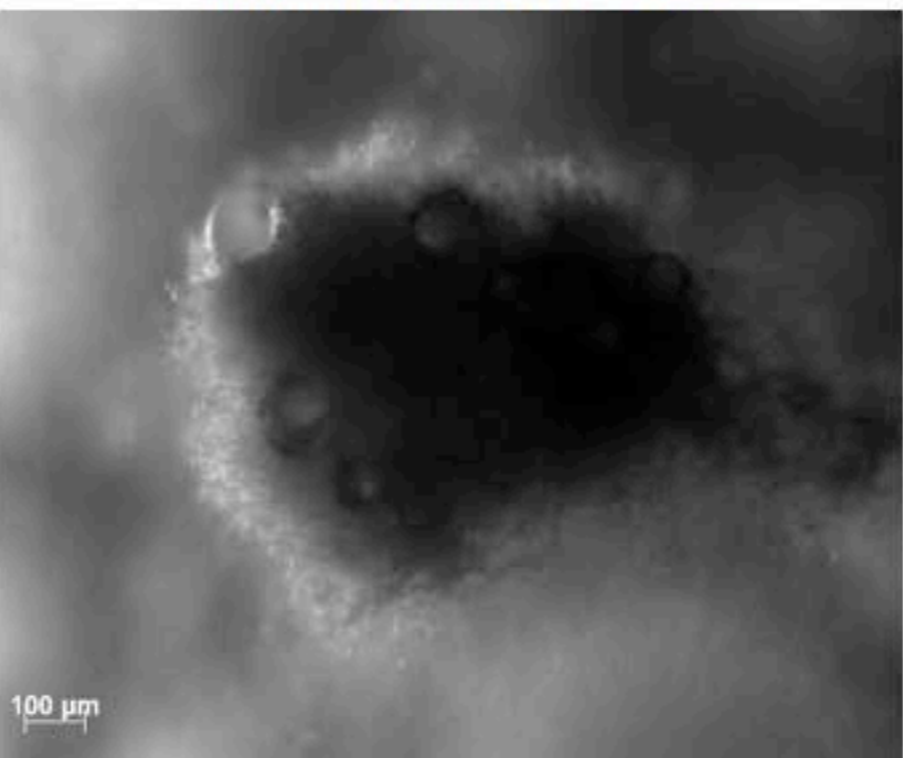
Streptomyces sp. HF17

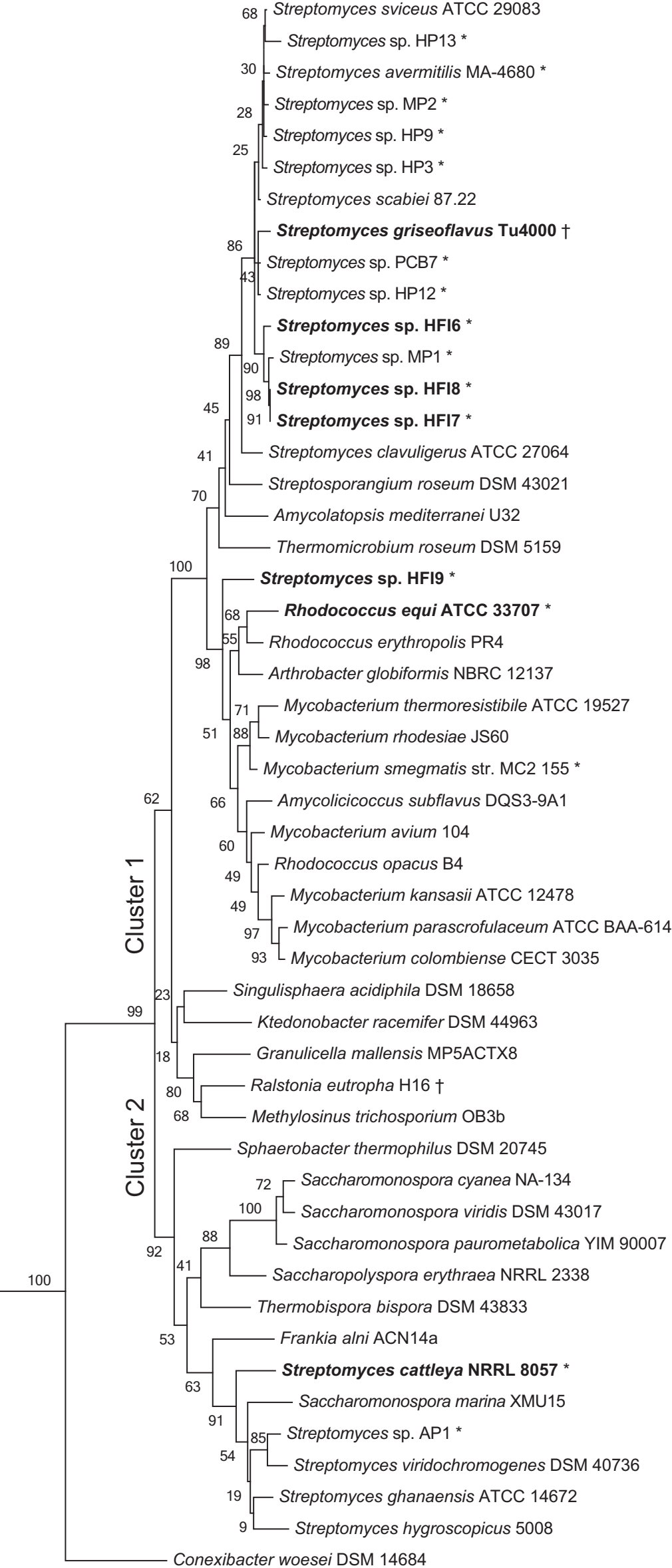


Streptomyces sp. HF18



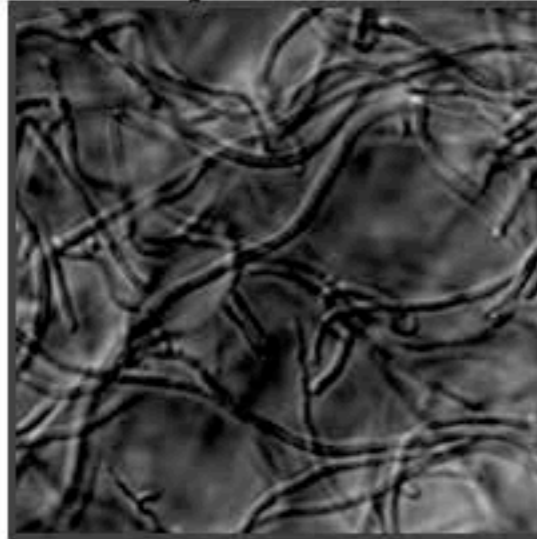
Streptomyces sp. HF19



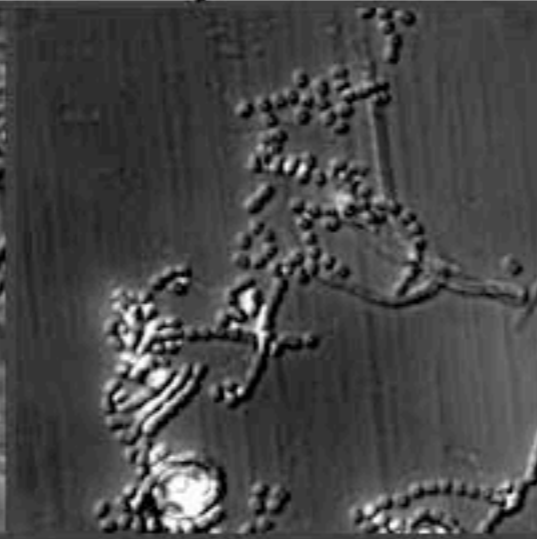


Streptomyces sp. HF18

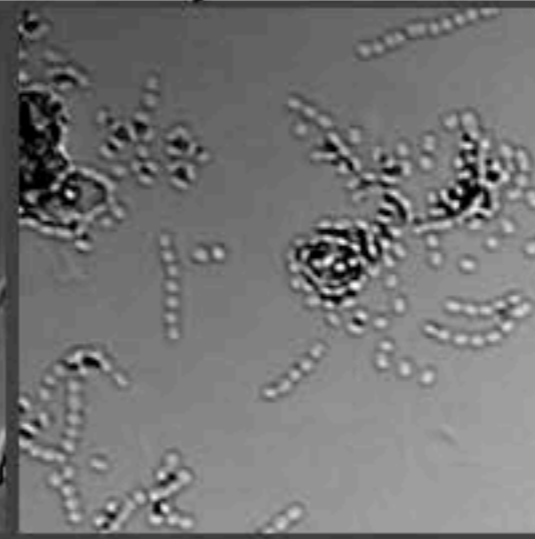
B : Day 1.1



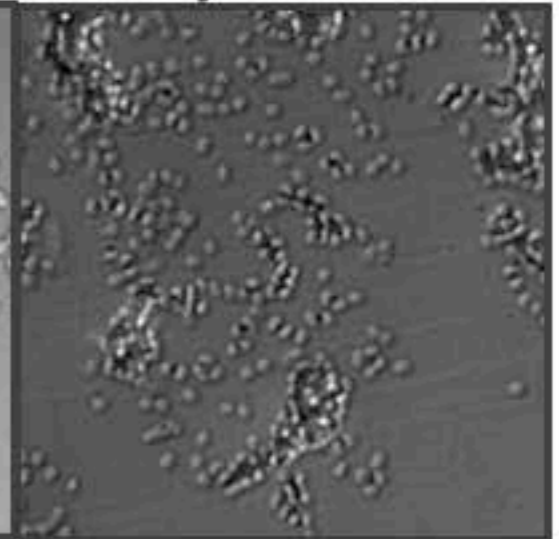
C : Day 1.8



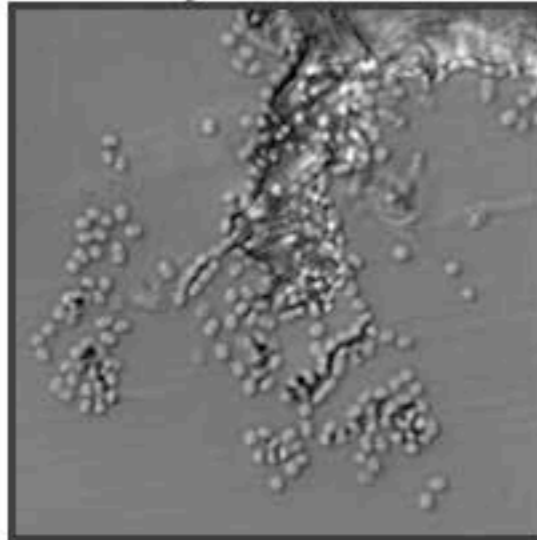
D : Day 2.9



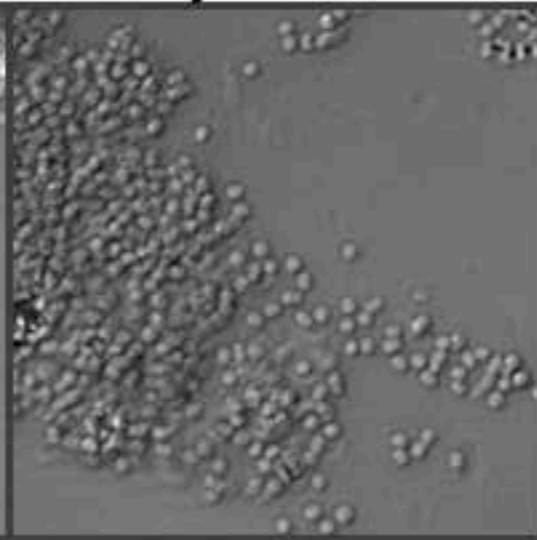
E : Day 3.8



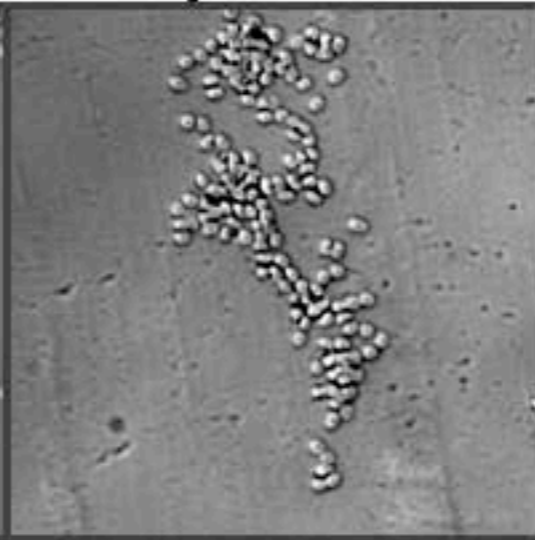
F : Day 6.1



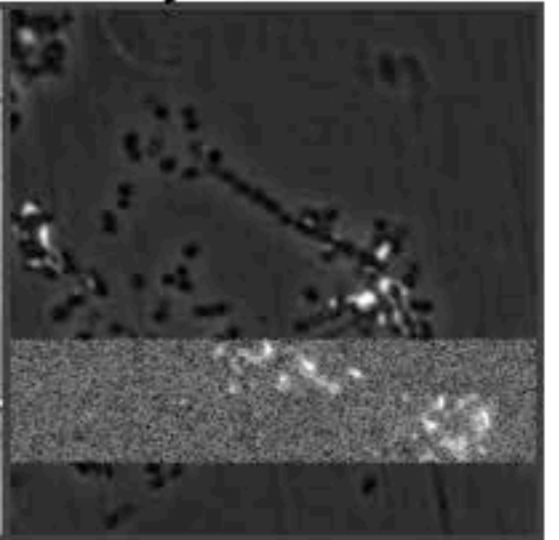
G : Day 8.1



H : Day 13.8



I : Day 22.0



10 μ m

a

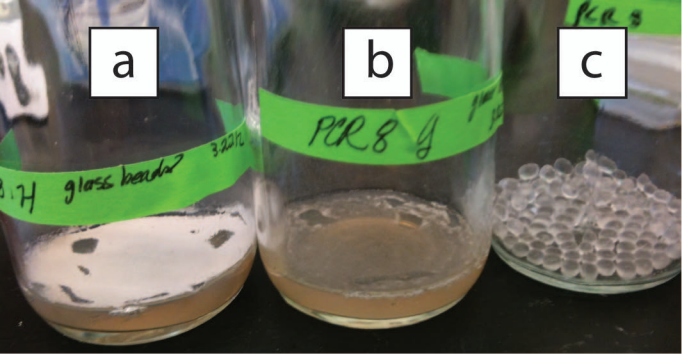
H. H glass beads 3.22 μm

b

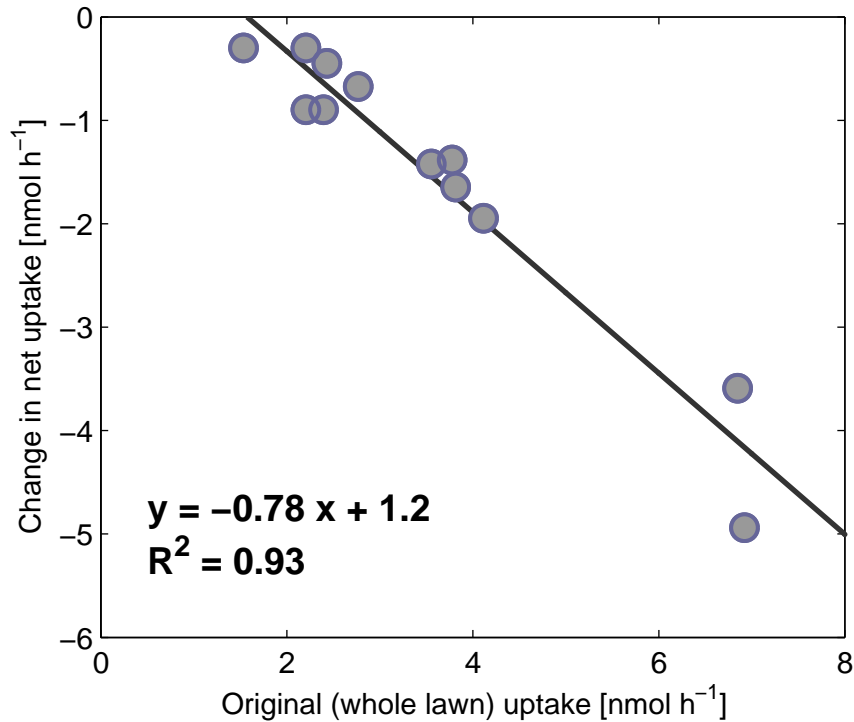
PCR 8 g

c

PCR 8 g

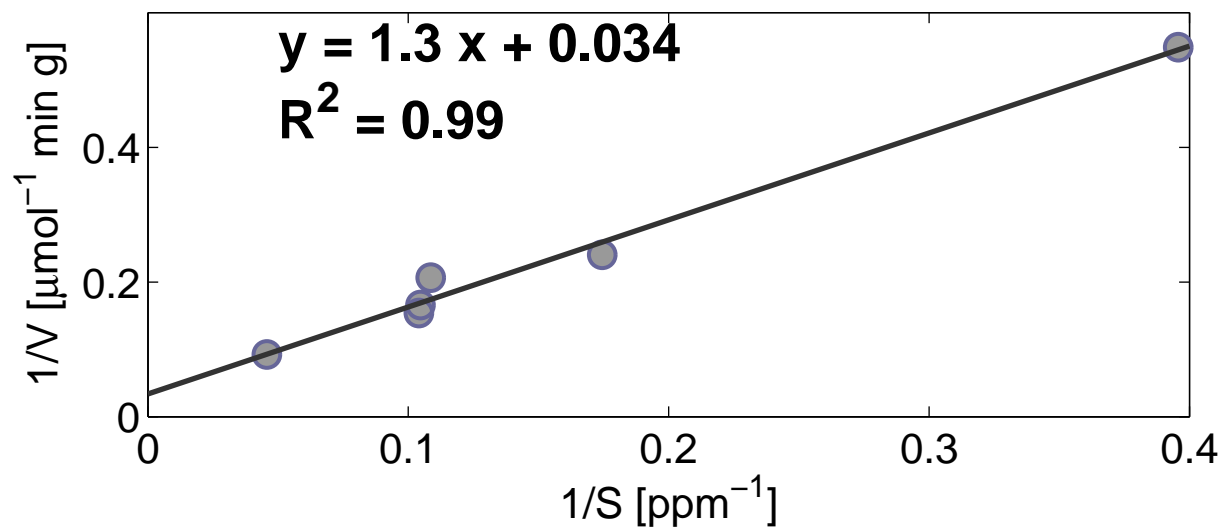


Loss in H₂ uptake by disturbance depends on original uptake



Kinetic Parameter Determination for Strain HFI8

Lineweaver-Burk Plot



Eadie-Hofstee Plot

